SELECTED METHODS OF GROUND IMPROVEMENT FOR AUSTRALIAN TRANSPORT INFRASTRUCTURE

Buddhima Indraratna[1], Ana Heitor[2], Cholachat Rujikiatkamjorn[3] and Rui Zhong[4]

[1]*Distinguished Professor, Research Director, Centre for Geomechanics and Railway Engineering, University of Wollongong*

[2]*Lectuer, Centre for Geomechanics and Railway Engineering, University of Wollongong*

[3]*Associate Professor, Centre for Geomechanics and Railway Engineering, University of Wollongong*

[4]*Research Fellow, Research Director, Centre for Geomechanics and Railway Engineering, University of Wollongong*

ABSTRACT

In coastal regions of Australia, high population densities and increased traffic have led to a substantial expansion of transportation infrastructure. These developments have necessitated the use of ground improvement techniques in response to environmental legislation and the need for sustained performance. In this paper, a brief overview of innovative ground improvement techniques in major areas such as railway embankments, port reclamation, and landfill operations is provided. Ballasted rail tracks are often placed on freshly quarried aggregate because it is resilient enough for cyclic and impact loads. However, ballasted layers often need periodic maintenance due to deformation and degradation, and while recycled ballast is a cheaper and environmentally viable option, its strength must be investigated beforehand, and different types of geosynthetics to improve the stability and drainage of railway tracks under high cyclic loading also need assessing. Field tests to measure the in-situ stresses and deformations of ballast have been carried out on sections of instrumented heavy haul track at Bulli and Singleton. Stabilization of soft subgrade soils using prefabricated vertical drains (PVDs) and stone columns is also needed to improve the overall stability of track and reduce differential settlement during operation. The effectiveness PVDs can be seen via field measurements and finite element analyses. Due to an increase in trade activities at the Port of Brisbane, Queensland (Qld), new facilities on Fisherman Islands at the mouth of the Brisbane River were constructed (reclamation) on the new outer area (235ha) adjacent to the existing port facilities. A vacuum assisted surcharge load and conventional surcharge scheme in conjunction with PVDs helped to reduce the required consolidation time through the deeper subsoil layers. The design of this combined vacuum and surcharge fill system and construction of the embankment are described in this paper. A 45 ha reclamation at the Outer Harbour extension of Port Kembla in Wollongong, NSW, gave us the opportunity to examine the potential use of coal wash (CW) and steel furnace slag (SFS) as predominant reclamation fill, while laboratory investigations indicated that an optimum CW-SFS mixture would meet most of the geotechnical specifications needed for an effective structural fill. A field application at Penrith Lakes, NSW, of a new methodology using the shear wave velocity (V_s) (i.e. Multichannel Analysis of Surface Waves MASW) and matric suction (u_a-u_w) or moisture content was investigated. The laboratory results and the results from preliminary field testing indicate that Vs and (u_a-u_w) trends could predict the compaction characteristics of the soil. The use of sustainable approaches for ground improvement such as bio- engineering, and recycled tyres with waste granular material, is also presented and discussed in this paper.

1 INTRODUCTION

Ground improvement techniques have been developed in Australia to suit a wide range of railway embankment conditions and reclamation projects. This paper focuses on new ground improvement techniques for transportation infrastructure within an urban environment. Since ballasted rail tracks are the largest transportation infrastructure in Australia that cater for public and freight transport, railway industries face challenges to improve their efficiency and decrease the cost of maintenance and infrastructure costs because the large cyclic stresses from heavier and faster trains induce large deformations and degradation of the ballast layer. While some previous researchers highlighted ballast breakage and confining pressure as key parameters in the design of ballasted rail tracks (Marshal 1973, Indraratna *et al*. 2005, Lackenby *et al*. 2007), and the potential use of bio engineering, geosynthetics, recycled tyres and waste aggregate to improve track stability is observed in several laboratory studies (Selig and Waters 1994, Raymond 2002, Indraratna and Salim 2003, Indraratna *et al*. 2010a), only a few have assessed the relative merits of geosynthetics and shock mats under *in situ* track conditions. Moreover, the 'field' performance of different types of geosynthetics to improve the overall stability of ballasted rail tracks has not been investigated systematically, so two extensive field studies have been carried out to fill this gap; this paper discusses the field instrumentation, monitoring processes, and the preliminary findings of these unique studies.

Many coastal regions of Australia contain very soft clays (estuarine or marine) which have low bearing capacity and high compressibility, so without appropriate ground improvement (Indraratna and Redana 1998; Bergado *et al*. 2002; Indraratna *et al*. 2009), excessive settlement and lateral movement would adversely affect the stability of buildings, ports, and transport infrastructure such as highways and rail embankments built on such soft ground (Holtz *et al*. 1991, Indraratna and Redana 2000). Constraints such as restricted space, tight construction schedules, environmental and safety issues, maintenance costs, and the longevity of earth structures continue to demand unfailing innovation in the design and construction of essential infrastructure on soft clays. The behavior of soft clay foundations stabilized with stone columns or a combination of vertical drains and vacuum pressure can now be predicted with acceptable accuracy due to the progress made over the past decade through rigorous analytical and numerical analysis. Mohamedelhassan and Shang (2002) proposed an analytical solution for one-dimensional consolidation with vacuum application, while Indraratna *et al*. (2005) extended the unit cell radial consolidation theory for vacuum application with instantaneous loading considering vacuum loss along the drain length. Indeed, without appropriate ground improvement, soft clays can sustain high excess pore water pressures (PWPs) during repeated loading. In response, this paper presents the design methodology and finite element analysis of a rail track stabilized with relatively short prefabricated vertical drains (PVDs); it shows that these relatively short, 6-8metre long PVDs could dissipate train induced pore pressures, limit lateral movement, and increase the shear strength and bearing capacity of this soft formation.

Coal wash (CW) and steel furnace slag (SFS) are by-products of the coal mining and steel industries, and as such are typically treated as wastes and disposed of in stockpiles that occupy usable land in urban areas. Effective recycling of these granular wastes through large-scale civil engineering applications such as reclamation and/or back-fill materials is vital for the local environment and the economy, however, given their heterogeneity and complex behavior under submerged conditions such as harbor reclamation fill, the design and construction utilizing these wastes poses significant geotechnical challenges. Moreover, fill areas such as Penrith Lakes, New South Wales (NSW), Australia are deemed to be uncontrolled fill due to insufficient compaction records, which is why a new methodology which combines MASW techniques and field matric suction is used to assess the quality of previously compacted areas. In this context, detailed laboratory investigations and preliminary field trials are reported.

2 SOFT SOIL STABILISATION

Fill surcharge (embankment) preloading is a proven technique for improving the shear strength of low-lying areas because it induces most of the ultimate settlement expected to be borne by soft ground after construction (Richart 1957; Indraratna and Redana 2000; Indraratna et al. 2005a). To avoid shear failure in the ground, a surcharge embankment is usually raised in multiple stages, with a rest period between each stage (Jamiolkowski et al. 1983) to allow excess pore pressure to dissipate. Since most compressible low-lying soils are very thick and have very low permeability, they often take a long time to consolidate, a situation that may be impractical if stringent construction schedules and deadlines are to be met. When PVDs and a surcharge are applied, the drainage path in a radial direction is shorter because the vertical drains reduce the necessary preloading period and thus reduce the risk of ground failure. Apart from PVDs, vacuum pressure is also used to enhance soft soil stabilisation, especially when a desired degree of consolidation is required over a relatively short time. Negative pore pressures (suction) distributed along the drains and on the surface of the ground accelerate consolidation, reduce outward lateral displacement, and increase the effective stress; this reduces the height of the surcharge embankment needed to prevent any instability and excessive outward lateral movement in the soil.

2.1 PLANE STRAIN CONVERSION

Plane strain finite element analysis can be readily adapted for a numerical simulation of multi-drain cases to most field situations (Bergado and Teerawattanasuk, 2008; Hird et al, 1992; Indraratna and Redana 2000; Indraratna et al. 2005a), but realistic field predictions mean that the axi-symmetric properties must be converted to an equivalent 2D plane strain condition, usually by modifying the permeability coefficients or drain geometry. Indraratna et al. (2005b) proposed an equivalent plane strain approach to simulate vacuum pressure for a vertical drain system, as shown in Figure 1.

Equivalent plane strain conditions can be achieved using: (1) a geometric approach where the PVD spacing changes and the soil permeability remains constant; (2) a permeability approach where the equivalent permeability coefficient changes while the drain spacing remains unchanged; (3) a combined permeability and geometric approach where plane strain permeability is calculated based on convenient drain spacing.

Indraratna et al. (2005b) proposed an average degree of consolidation for plane strain by assuming that the plane strain cell (width of 2*B)*, the half width of the drain b_w and the half width of the smear zone b_s are the same as their axi-symmetric radii r_w and r_s, respectively. By making the magnitudes of R and B the same, Indraratna et al. (2005a) presented a relationship between k_{hp} and k'_{hp}.

The smear effect can be captured by the ratio between the smear zone permeability and the undisturbed permeability, hence:

$$\frac{k'_{hp}}{k_{hp}} = \frac{\beta}{\frac{k_{hp}}{k_h}\left[\ln\left(\frac{n}{s}\right) + \left(\frac{k_h}{k'_h}\right)\ln(s) - 0.75\right] - \alpha} \tag{1}$$

where k_{hp} and k'_{hp} are the equivalent undisturbed horizontal and corresponding smear zone permeability, respectively.

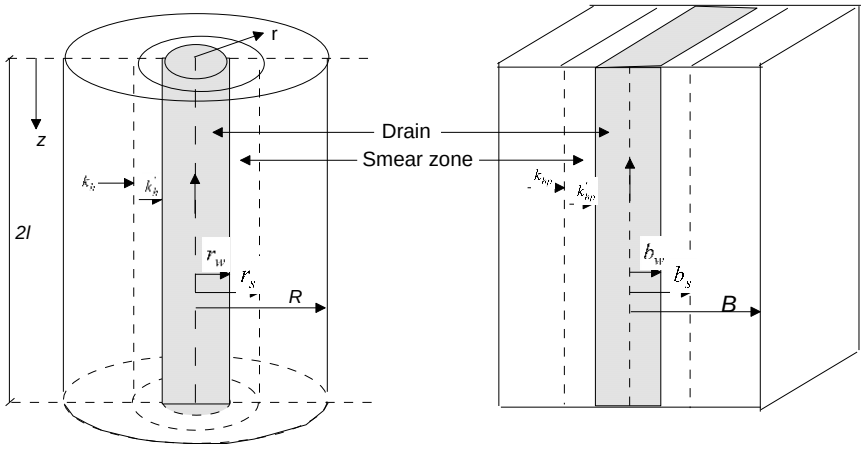

(a) Axisymmetric (b) Plane strain

Figure 1: Conversion of an axisymmetric unit cell into a plane strain condition (Indraratna et al. 2005b, with permission from ASCE)

The geometric parameters α and β are given by:

$$\alpha = \frac{2}{3} - \frac{2b_s}{B}\left(1 - \frac{b_s}{B} + \frac{b_s^2}{3B^2}\right) \tag{2a}$$

$$\beta = \frac{1}{B^2}(b_s - b_w)^2 + \frac{b_s}{3B^3}\left(3b_w^2 - b_s^2\right) \tag{2b}$$

Indraratna et al. (2005b) compared two different distributions of vacuum along a single drain for the equivalent plane strain (2D) and axisymmetric conditions (3D). Varying the vacuum pressure in PVDs installed in soft clay would be more realistic for long drains, but a constant vacuum with depth is justified for relatively short drains.

2.2 PERFORMANCE OF PVD UNDER CYCLIC LOADING

Low lying areas with high volumes of plastic clays can sustain high excess pore water pressure during repeated cyclic loading. The ability of PVDs to dissipate cyclic pore water pressures has been discussed by Indraratna et al. (2009a). A large scale triaxial test is used to determine how a cyclic load affects radial drainage and consolidation by PVDs, using specimens 300 mm in diameter by 600 mm high. Excess pore water pressure is monitored via miniature pore pressure transducers which are saturated in distilled water with a vacuum pressure and then fitted to desired locations on the samples through the base of the cell. These tests can be carried out at frequencies of 5-10 Hz, typically simulating train speeds of say 60-100 km/h with 25-30 tonnes/axle train loads. Figure 2 shows the excess pore water pressure ratio R_u versus the number of cycles N in a series of three separate tests. Without a PVD the excess pore pressure increases rapidly ($R_u \approx 0.9$), and undrained failure also occurs rapidly. The corresponding axial strains are shown in Figure 3a. Without a PVD, large cyclic axial strains develop and failure occurs rapidly after about 200 cycles in the cyclic CK_0U test, and almost 100 cycles in the cyclic UC (cyclic confined compression) test. As Figure 3b shows, failure occurs when $\varepsilon_a - \log N$ curves begin to concave rapidly downwards. With a PVD, the axial strain gradually increases to a stable level and there is no failure, even after 3,000 cycles. The tests indicate that PVDs can decrease the excess pore pressure induced by cyclic loading, and soft clays where radial drainage is helped by PVDs can be subjected to higher cyclic stress levels than the critical cyclic stress ratio without causing undrained failure.

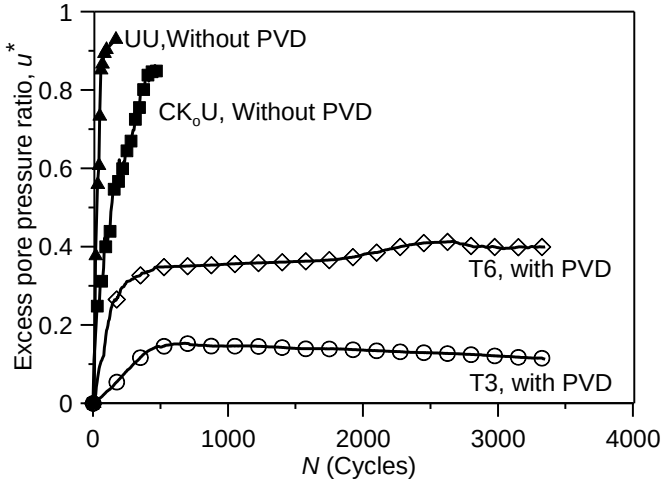

Figure 2: Excess pore pressure under cyclic loading with and without PVD (Indraratna et al. 2009a, with permission from ASCE)

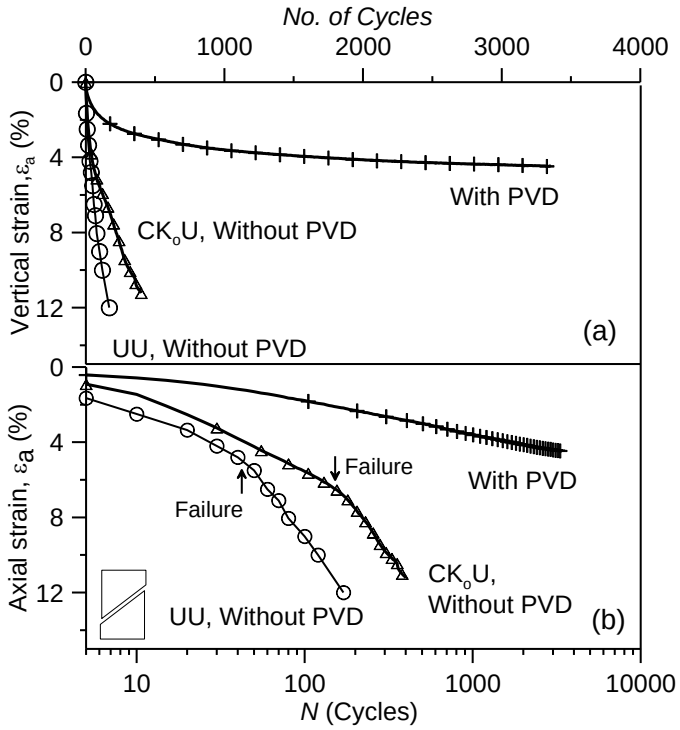

Figure 3: Axial strains during cyclic loading with and without PVD: (a) arithmetic; (b) semi logarithmic scales (Indraratna et al. 2009a, with permission from ASCE)

2.3 CASE STUDY

The Pacific Highway linking Sydney and Brisbane was constructed to alleviate the traffic congestion in Ballina. This bypass route had to cross a floodplain consisting of highly compressible and saturated marine clays up to 40 m thick, and where the groundwater is almost at the ground surface. The water content of this soft and medium silty clay varies from 80 to 120%, which is generally at or exceeds the liquid limit, thus ensuring these soils are fully saturated. Field vane shear tests indicate a shear strength ranging from 5-40 kPa, while standard oedometer testing revealed a compression index ($C_c/(1+e_0)$) between 0.30-0.50. A system of vacuum assisted surcharge load in conjunction with PVDs was chosen to shorten the consolidation time and stabilise the deeper layers of clay, and to determine its effectiveness, a trial embankment was built north of Ballina, into which 34mm diameter circular PVDs at 1.0m spacing are installed in a square pattern. The vacuum system consists of PVDs with an air and water tight membrane, horizontal transmission pipes, and a heavy duty vacuum pump. Transmission pipes are laid horizontally beneath the membrane to

distribute the vacuum uniformly, and the boundaries of the membrane are embedded in a peripheral trench filled with soil-bentonite to ensure absolute air tightness. Figure 4 shows where the instruments are positioned, including the surface settlement plates, inclinometers and piezometers. The piezometers are placed 1m, 4.5m, and 8m below the ground level, and eight inclinometers are installed at the edges of each embankment. The embankment area is divided into Section A (with no vacuum pressure), and Section B, which is subject to vacuum pressure and surcharge fill. Since the layers of soft clay vary between 7m to 25 m thick, the embankment varies from 4.3m to 9.0m high, to limit the post-construction settlement. A vacuum pressure of 70 kPa was applied at the drain interface and removed after 400 days.

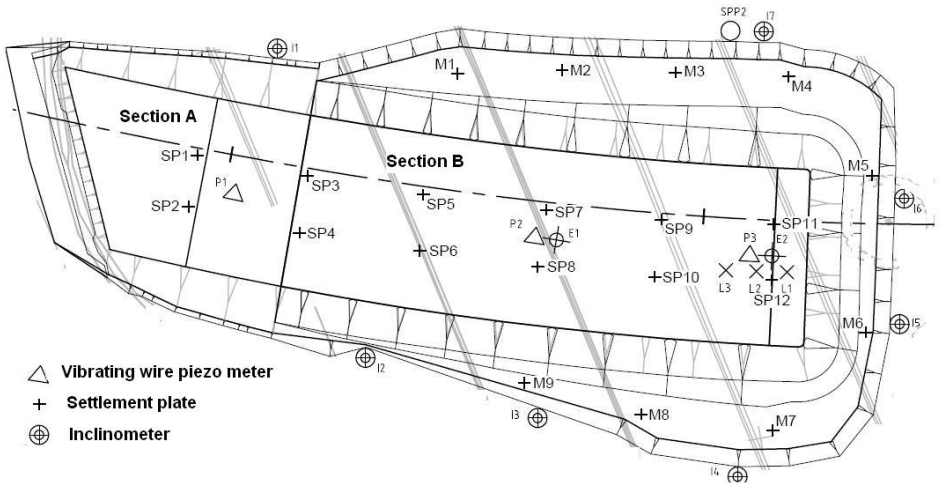

Figure 4: Layout of the instrumentation t for the test embankments at Ballina Bypass (Indraratna et al. 2009b)

Figure 5 shows the settlement and associated pore pressure recorded by the settlement plates and piezometers, as well as a history of embankment construction. The actual suction varies from -70 kPa to -80 kPa, and there are no air leaks. 2D and 3D single drain analyses are used to compute settlement at location SP-12. The construction history and settlement measured at settlement plate SP-12 are shown in **Error! Reference source not found.**Fig. 6. Based on the CPT data, the clay here is assumed to be 24m thick. The predictions from the plane strain and axisymmetric analyses agree with the measured data, and the rate of settlement increased significantly after a vacuum is applied (Fig. 6b).

Vacuum assisted consolidation is an innovative method recently and successfully used for large scale projects on very soft soils in reclamation areas; here the fill surcharge is reduced to achieve the same amount of settlement and lateral displacement as soft soil consolidated by PVDs used with vacuum pressure. This system depends on (a) the air tightness of the membrane, (b) the seal between the edges of the membrane and the ground surface, and (c) the soil conditions and location of the ground water level. Analytical modelling of vertical drains with vacuum preloading under axi-symmetric and plane strain conditions that simulate the consolidation of a unit cell surrounding a single vertical drain is now a reality, and these simplified plane strain methods can be readily incorporated into finite element analysis. To convert from 3D to 2D based on a correct transformation of permeability and vacuum pressure, ensure that the time-settlement curves are the same as the true 3D analysis. Apart from road embankments, PVDs will also help stabilise rail tracks in coastal areas containing a high percentage of clayey subgrades. Moreover, short PVDs can be used under rail tracks to improve stability by dissipating excess cyclic pore pressure and curtailing lateral displacement.

3 STONE COLUMNS FOR TRANSPORT INFRASTRUCTURE IN SOFT SOILS

Installing stone columns into soft ground increases it's bearing capacity and accelerates consolidation (Basack et al. 2015a), and since foundations supporting transport infrastructure are subjected to cyclic loading, the specific aims of this project are to quantify the load displacement and consolidation characteristics, optimise column installation, and incorporate the influence of high frequency cyclic loads.

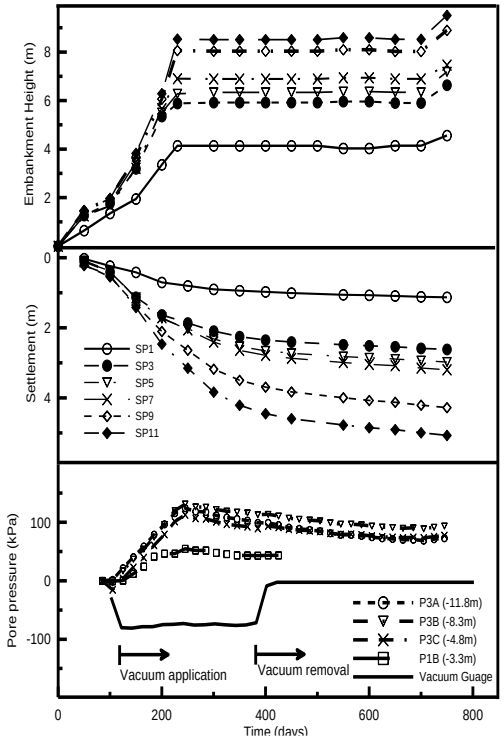

Figure 5: Embankment stage construction with associated settlements and excess pore pressures (Indraratna et al. 2009b)

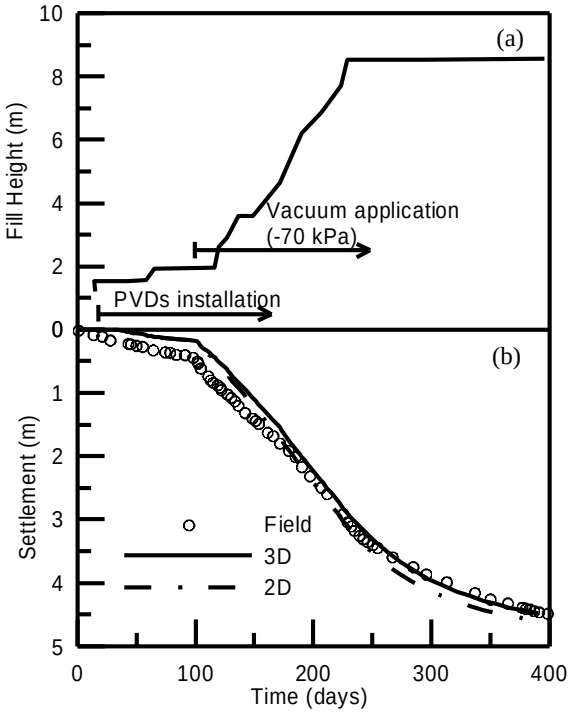

Figure 6: (a) loading history; and (b) consolidation settlements for settlement plate SP-12 (Indraratna et al. 2009b)

The load transfer and consolidation characteristics of stone columns are captured by advanced analytical and numerical modelling (Indraratna *et al.* 2013) based on unit cell analogy and free strain hypothesis. The distribution of vertical stress in soft soil is quantified by the following equation:

$$w(r) = w(r_e) + (N - r/r_c)^2 F(N, n_s) \tag{3}$$

where r = radial coordinate, r_c & r_e = column and unit cell radii, $N = r_e / r_c$.

The radial consolidation characteristics of soft ground are governed by Barron's Equation for radial consolidation coupled with the modified Cam-clay theory (Basack *et al.* 2015*b*). The lateral deformation of columns is quantified by stress-induced deformation (ρ_z^e) and the barrelling component (ρ_z^s). The governing equations are as follows:

$$\rho_z^e = \frac{\mu_c r_c}{E_c}\left[\sigma_z^v + \left(1 - \frac{1}{\mu_c}\right)\sigma_z^r\right] \tag{4}$$

$$\rho_z^s = \xi(z^2 - Hz) + \rho_z^e \frac{z}{H}(1 - \eta_b) + \rho_z^e \left(1 - \frac{z}{H}\right)(1 - \eta_t) \tag{5}$$

$$\int_0^H \rho_z^s \left(r_c + \frac{\rho_z^s}{2}\right) dz = 0 \tag{6}$$

where μ_c and E_c are the Poisson's ratio and elastic modulus of the column, σ_z^v and σ_z^v are the vertical and radial column stress components at depth z, H is the thickness of soft soil, and ξ, η_t and η_b are the appropriate non-dimensional coefficients. A comparison of the computed results with field data (Fig.7) indicates that the analysis is accurate. Discrete element modelling (DEM) using PFC^{-3D} software has been carried out (Indraratna *et al.* 2014), by idealizing the stone particles as rounded and sub-rounded spherical clumps (Fig.8). A comparison of the DEM results with the physical test results (Sivakumar *et al.* 2011) indicates consistent modelling (Fig.9).

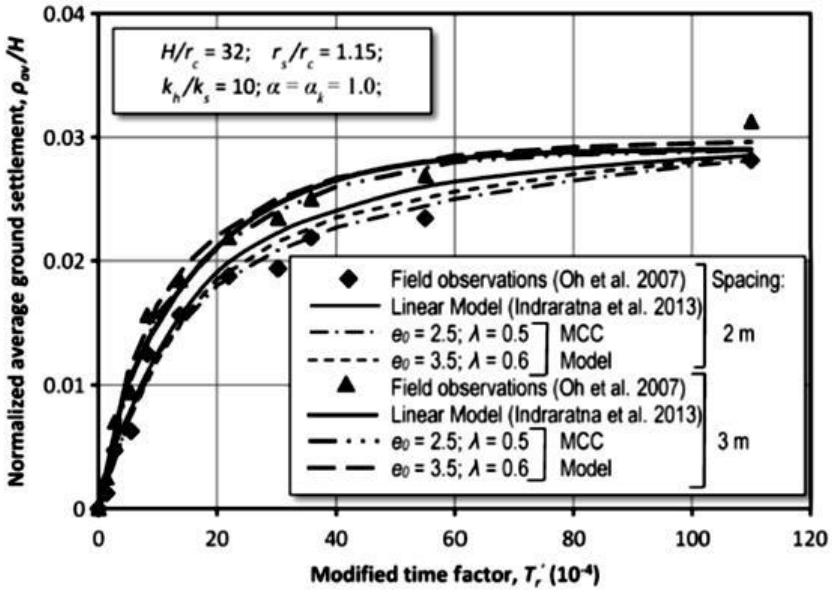

Figure 7: Comparison of numerical results with field data (with kind permission from ASCE)

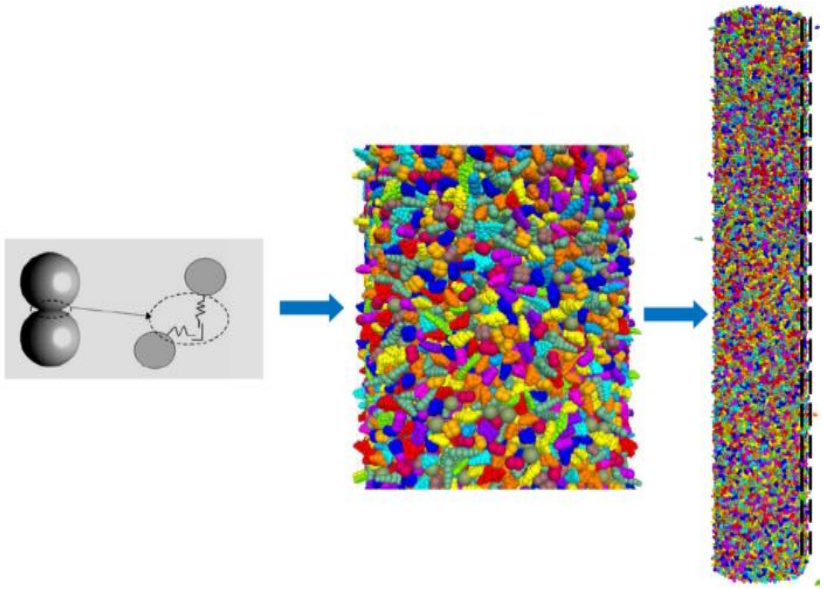

Figure 8: DEM simulation of column particles

3.1 LABORATORY TEST OF A SINGLE COLUMN

Large-scale one-dimensional consolidation tests on instrumented single stone column in soft kaolin clay have been carried out and indicate that the stress concentration ratio is influenced by time and the particle size distributions. A post-consolidation exhumation of the column and then a CT-scan image quantified the lateral deformation and intrusion of fines (Fig.10). The performance of this reinforced soft soil depended largely on particle morphology and reinforcement geometry.

3.2 INFLUENCE OF CYCLIC LOADING

The behaviour of stone column reinforced soft ground under sinusoidal cyclic loading is being studied using yield surface contraction that incorporates the appropriate degradation functions. A comparison between the preliminary results with laboratory test data (Fig. 11) of Indraratna et al. (2009) and solutions of Ni (2012) implies that this analysis is acceptable.

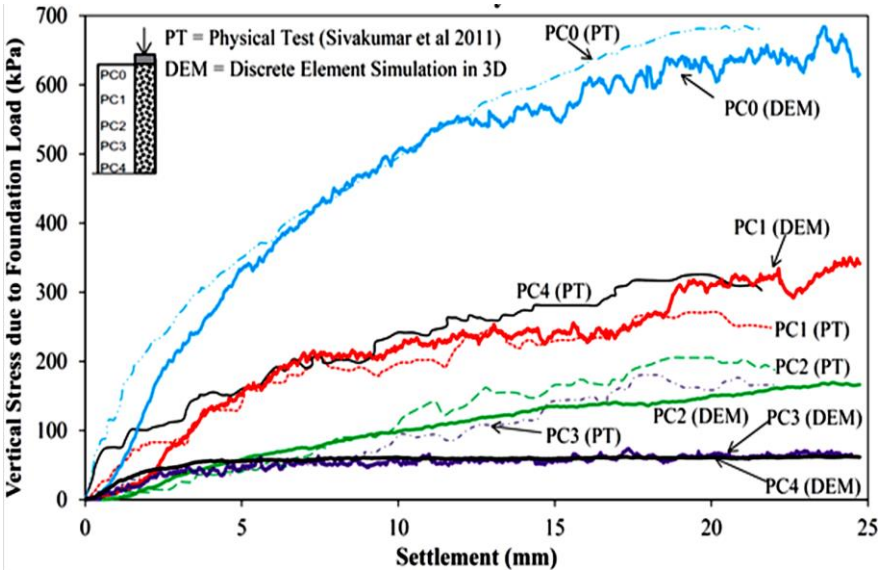

Figure 9: Comparison of DEM versus test results

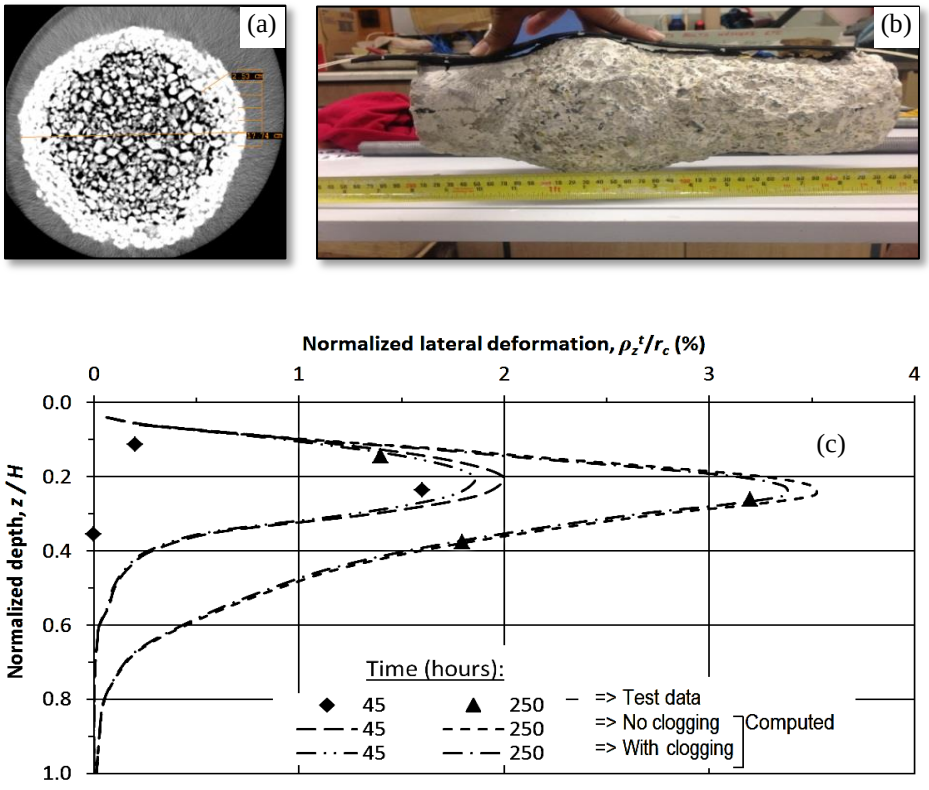

Figure 10: (a) CT-scan image of column cross section, (b) exhumed column, and (c) lateral deformation-depth plot

In summary, the stress concentration ratio depends on the time, depth, and PSD. Clogging retards the overall consolidation process, and the degree to which the strength and stiffness of soil is improved depends on the column geometry, ground conditions, and the loading pattern. The lateral deformation of a column varies with time and depth, whereas the build- up of pore water pressure by cyclic loading increases with the number of cycles, which means this rise, depends on the loading frequency, amplitude, and initial consolidation.

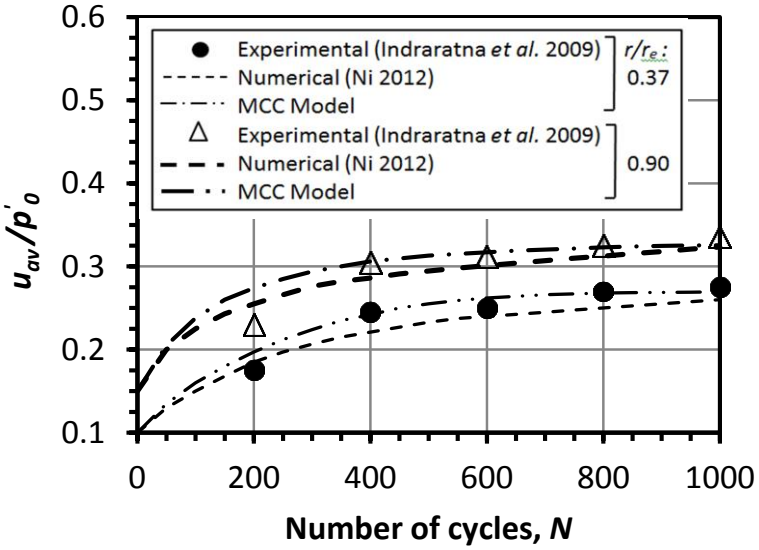

Figure 11: Cyclic loading analysis

4 USE OF GEOGRIDS AND GEOCELLS FOR RAIL TRACKS

Geosynthetics have been widely and successfully used in new rail tracks and in track rehabilitation schemes for almost three decades and when appropriately designed and installed, are a cost effective alternative to traditional techniques (Selig and Waters 1994). The application of geosynthetics for railway construction can be categorised into: (i) separation, (ii) reinforcement, (iii) filtration, (iv) drainage and, (v) moisture barrier/waterproofing. Geocomposites can reinforce the ballast and provide simultaneous filtration and separation functions (Rowe and Jones 2000); in fact a combination of reinforcement by geogrid and the filtration and separation provided by bonded non-woven geotextile will reduce lateral spreading, fouling, and degradation, especially in wet conditions (Ngo et al. 2014; Indraratna et al. 2011a). Non-woven geotextile also prevents fines from moving up from the subballast and subgrade (subgrade pumping), thereby keeping recycled ballast relatively clean. Given the complex behaviour of composite track systems consisting of rails, sleepers, ballast and sub-ballast under repeated traffic loads, current track design techniques are overly simplified (Indraratna et al. 2011b). To examine the potential benefits of geosynthetics in rail track, a field study has been carried out on a 60m long section of instrumented track built between two turnouts at Bulli along the coast of New South Wales, north of Wollongong city. This track is divided into four, 15m long sections, two of which have no geocomposite layer, while the remaining sections have a geocomposite layer beneath the fresh and recycled ballast (Indraratna et al. 2010). A typical cross section of this track is shown in Figure 12.

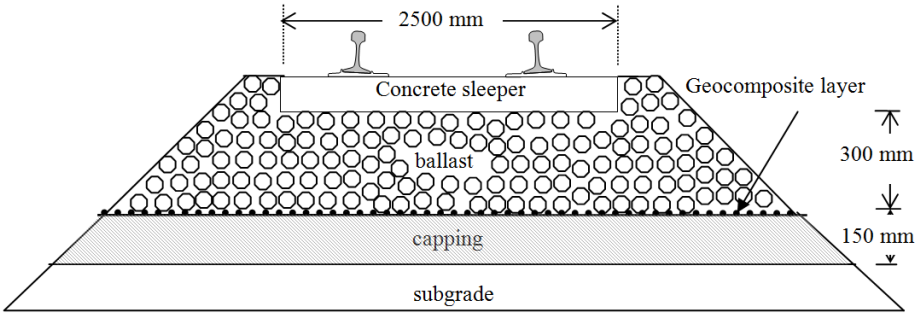

Figure 12: Section of ballasted track bed with geocomposite layer at the ballast-capping interface

The overall thickness of this bed is 450 mm, and it consists of a 300m thick layer of ballast and a 150mm thick capping layer. The particle size, gradation, and other index properties of this ballast are in accordance with Technical Specification TS 3402 (Railcorp, Sydney), which represents sharp angular coarse aggregates of crushed volcanic basalt (latite). Recycled ballast comes from a recycled plant at Chullora yard near Sydney. Table 1 presents the particle size distributions of fresh ballast, recycled ballast, and the capping materials used in this instrumented track (Indraratna et al.

2011a). There are bi-axial geogrids over the non-woven polypropylene geotextile which act like the geocomposite layer installed at the ballast-capping interface. The technical specifications of geogrid material used at the site can be found elsewhere (Indraratna et al. 2013).

The performance of this track under repeated wheel loads is monitored with sophisticated instrumentation; its vertical deformation was measured by settlement pegs, and lateral deformation was measured by electronic displacement transducers. The settlement pegs and displacement transducers were situated at the sleeper-ballast and ballast-subballast interfaces, and the pressure cells and displacement transducers were connected to a computer controlled data acquisition system.

Table 1: Grain size characteristics of fresh ballast, recycled ballast and capping materials (Indraratna et al. 2011a)

Material	Particle shape	d_{max}(mm)	d_{min}(mm)	d_{50}(mm)	C_u	C_c
Fresh Ballast	Highly angular	75.0	19.0	35.0	1.5	1.0
Recycled Ballast	Semi-angular	75.0	9.5	38.0	1.8	1.0
Capping	Angular to rounded	19.0	0.05	0.26	5.0	1.2

4.1 AVERAGE VERTICAL AND LATERAL DEFORMATION OF THE BALLAST LAYER

To investigate the overall performance of the ballast layer, the average vertical deformation $(S_v)_{avg}$ is considered by using the mean of measurements taken from under the rail and the edge of the sleeper at each interface. The values of $(S_v)_{avg,}$ are plotted against the number of load cycles (N) in Figure 13a and in recycled ballast they are smaller than for fresh ballast. The recycled ballast can benefit from less breakage because they are often less angular, which prevents corner breakage due to high contact stresses, and it is moderately-graded unlike the relatively uniform fresh ballast. With granular materials, an increased uniformity coefficient (C_u) leads to a more compact packing arrangement (i.e. reduced void ratio), so it is not surprising that the recycled ballast exhibits less displacement due to its higher C_u value than the fresh ballast, even though individual particles of recycled ballast are more rounded ($\phi = 43^0$-54^0) than the more angular fresh ballast ($\phi = 46^0$-69^0). At a given number of load cycles, the geocomposite inclusion leads to a decrease in the $(S_v)_{avg}$ of recycled ballast. Figure 13b shows the average lateral deformation $(S_h)_{avg}$ of ballast (i.e., measured from the average of lateral spreading at the sleeper-ballast and ballast-capping interfaces) plotted against the number of load cycles (N). Here the fresh ballast with geocomposite deforms less due to the highly frictional, angular particles of fresh ballast which develop an increased apparent friction with the geocomposite layer. The values of $(S_h)_{avg}$ of recycled ballast are less than the fresh ballast, and the recycled ballast stabilised with a layer of geocomposite exhibits values of $(S_h)_{avg}$ that are less than of the unreinforced fresh ballast (i.e. without geosynthetics); hence the inclusion of geocomposite is highlighted because it reduces the lateral spread of ballast; in practice, the confining and reinforcing properties of this geocomposite layer (i.e. geogrid bonded with the geotextile drainage layer) increases the lateral stability of ballast and also helps to reduce track maintenance (Indraratna et al. 2010). However, while this reduction in the lateral movement of ballast reduces the need for additional layers of crib and shoulder ballast during maintenance, if more internal confining pressure in the track could be provided by placing a geosynthetic layer within the ballast bed itself, then the lateral deformation of ballast would decrease substantially.

While the track substructure is essentially self-supporting with minimal lateral restraints, and the effective confining pressure is a key parameter governing the design of railway tracks because it has implications on the movement of ballast and associated track maintenance, an increase in track confinement due to geosynthetics is as significant as reducing the tamping, levelling and lining associated with ease of maintenance. Tracks deteriorate due to accumulated plastic settlement in the track layers, with serious consequences for passenger comfort, safety, and efficiency (speed restriction) during operation, which is why the ability of geosynthetics to prevent track deterioration is appealing to the railway industry; geosynthetics cost less in relation to the substantial savings generated by an extended track life-cycle and more resilient ballast behaviour (Indraratna et al. 2010).

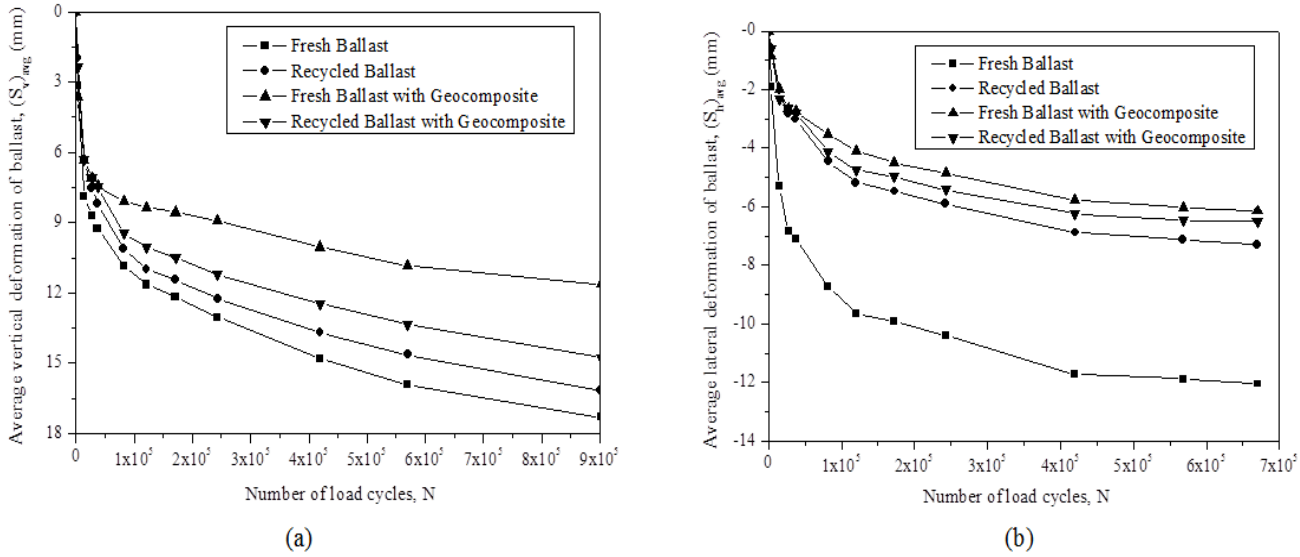

Figure 13: (a): average vertical deformation $(Sv)_{avg;}$ (b): average lateral deformation $(S_h)_{avg}$ of the ballast layer (modified after Indraratna et al. 2011a)

4.2 THE USE OF GEOCELL-REINFORCED SUBBALLAST

The granular layers in railroads such as ballast and sub-ballast spread laterally and undergo substantial differential settlement which leads to localised track failure (Selig and Waters 1994). Reinforcing the underlying subballast with geocells (a three-dimensional form of geosynthetics) is now a widely used economic and feasible alternative (Ngo et al. 2016). To investigate the performance of sub-ballast reinforced with geocells, a large-scale track process simulation apparatus (TPSA) is used (Figure 14). A stress controlled cyclic loading with a maximum cyclic stress of 166 kPa will provide the most critical type of the stress that can be applied to the sub-ballast (Biabani et al. 2016). To simulate a train travelling at relatively low to high speeds, frequencies of f = 10, 20 and 30 Hz are chosen, and relatively low confining pressures of σ′3 = 5, 10, 15, 20 and 30 kPa are used to mimic low confinement applied to actual tracks. To simulate the plane strain condition on a long and straight track, the vertical walls are free to move parallel to the tie, but cannot move perpendicular to the tie. All of these experiments continue for up to N = 500,000 cycles to characterise the long-term performance of geocell-reinforced subballast.

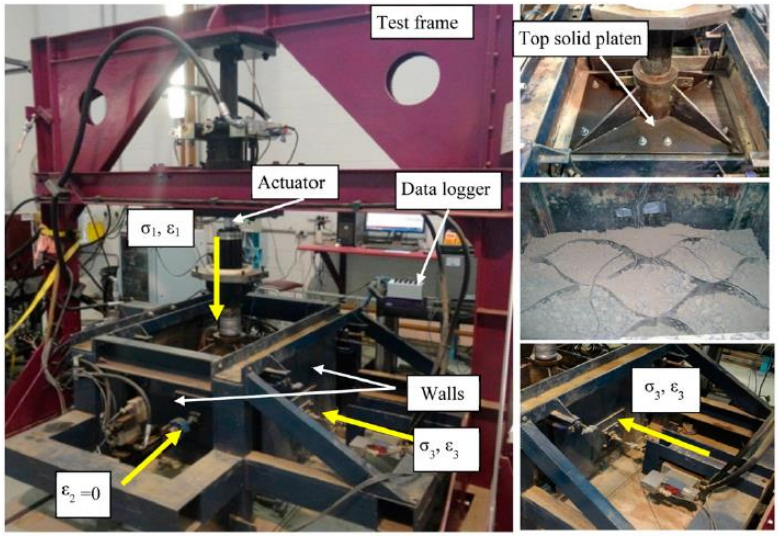

Figure 14: Track process simulation apparatus -TPSA (modified after Indraratna et al., 2015)

The beneficial effect of geocells is seen in terms of reducing the vertical strain. Figure 15a shows the variation of vertical strain ε_1 of unreinforced and geocell-reinforced sub-ballast versus different confining pressures (σ′3). The results show that utilising the geocell reduces vertical strains in the sub-ballast, particularly at a very low confining pressure because the infill soil is confined in the geocell pocket, which minimises lateral deformation. Figure 15a also

shows that the vertical strain increases as the frequency (f) increases; this shows how the frequency (or train speed) impacts on the behaviour of sub-ballast in unreinforced and reinforced conditions. The resilient modulus (M_R) is an important parameter that controls the resilience of granular materials; in this study the magnitude of M_R is determined by the ratio of cyclic stress and recoverable vertical strain. The results that M_R increases in magnitude the frequency of cyclic loading (Figure 15b) increases; this shows how frequency impacts on the acceleration of particle densification, which improves the MR. The value of M_R increases with an increase in the number of cycles (N). There is a marginal improvement beyond N ≥ 100,000 cycles, which exhibits a 'stable' zone. Laboratory data indicates that geocell has a definite beneficial effect when used to construct new tracks because it can support higher train speeds, and modernise existing tracks to reduce maintenance.

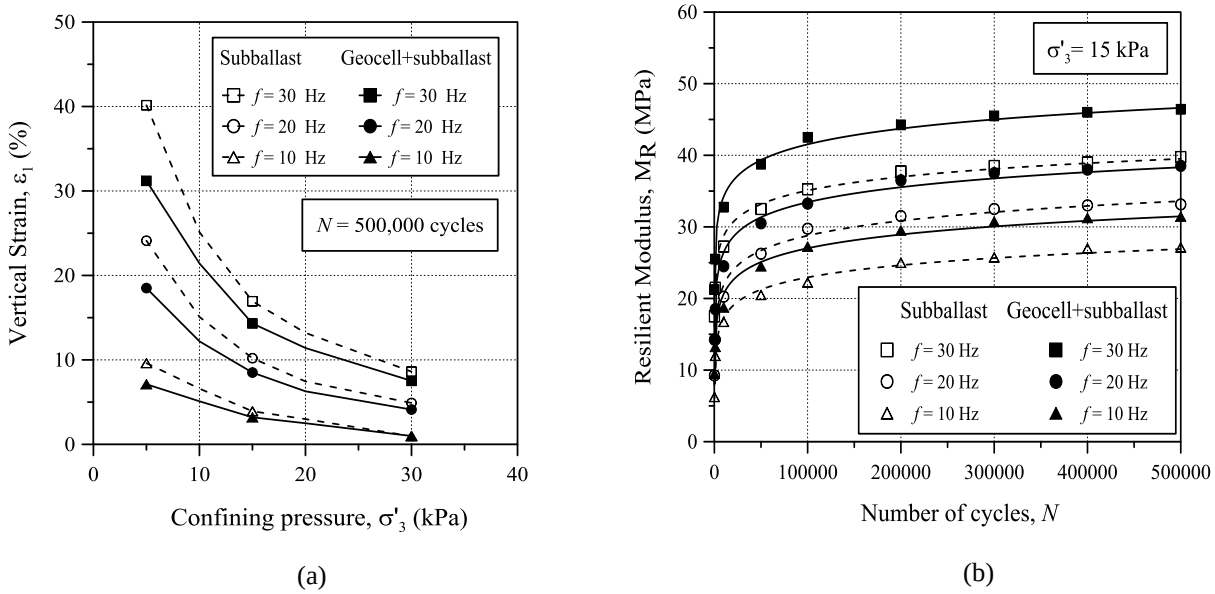

Figure 15: (a) Effect of` confining pressure on vertical strain, (b) Variation of resilient modulus at different number of cycles (N) (modified after Indraratna et al. 2015)

5 COMPACTION OF GRANULAR MATERIALS FOR PORT RECLAMATION AND LANDFILLS: CASE STUDIES

In line with the growing demand for imports and exports from Australia, port infrastructure has become an increasingly critical part of the country's growth because they are gateways for international and domestic freight to Australian markets. Port facilities in most Australian cities and major export hubs are already close to capacity, and the ability to expand these facilities is restricted by access to suitable adjacent land due to their proximity to urban areas. Owing to the limited availability of usable space and constraints associated with environmental and safety issues, maintenance costs and the longevity of geostructures, port expansion projects often rely on land reclamation, but these reclamation schemes mainly involve the use of dredged or borrowed materials that typically require additional improvement in order to achieve the required performance criteria.

5.1 CASE STUDY: PORT KEMBLA

Over the last decades Port Kembla Harbour has grown to accommodate the expansion of local industries such as the coal and steel export market. However, most of these activities have been in the Inner Harbour area, which is quickly approaching its capacity, so the port authority is now planning to develop the Outer Harbour (Fig. 16). This development will create more bulk cargo berths, which corresponds to approximately 45 hectares of reclaimed land.

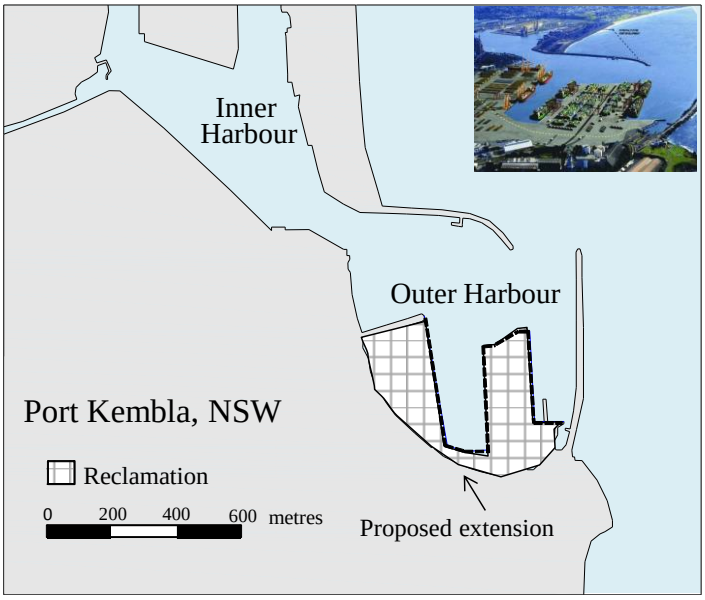

Figure 16: Illustration of the proposed extension area of the Port Kembla (Indraratna et al. 2015)

The type of reclamation fills used at Port Kembla would dictate a more important component of total settlement, apart from the obvious implications on its load bearing capacity. Therefore, to develop the Outer Harbour the PKPC will use a reclamation design that eliminates the need to remove any of the underlying dredged spoil, and they will only utilise passive preloading for ground treatment. If the foundations for port infrastructure are not properly stabilised, unacceptable settlement and sudden subsidence of these granular fills, as well as significant differential movements and lateral displacement can cause damage to the surface structures and the adjacent facilities (pipelines and retaining walls, etc.). Thus, it is vital to examine the geotechnical properties of the fills used in the reclamation.

The use of locally available granular waste materials (i.e. coalwash and steel furnace slag) as potential reclamation fills is an economical alternative to conventional (quarried) aggregates and dredged sandy fills because it has some benefits from the environmental sustainability viewpoint (Rujikiatkamjorn et al., 2013, Tasalloti et al., 2015a). However, improving heterogeneous waste materials such as slag and coalwash by compaction poses some challenges related to their adverse geotechnical properties, i.e. the breakage potential of coalwash (Levental and Ambrosis, 1985, Indraratna et al., 1994, Heitor et al., 2016) and the volumetric instability (swelling) of steel furnace slag (Wang, 2010, Heitor et al., 2015). To examine the geomechanical behaviour of these granular waste materials, they underwent a compaction field trial.

5.1.1 Materials

Coalwash (CW) is a by-product from a washery process that refines run-of-mine (ROM) coal. For every metric tonne of ROM coal that enters a washery plant, approximately 200kg of the output consists of granular waste material, of which 80% corresponds to coarse-grained coalwash and 20% as fine-grained tailings. Coal mining operations in Australia alone generate a several hundreds of millions of tonnes of coal wash per year (Leventhal and de Ambrosis, 1985). Steel furnace slag (SFS) is a by-product of steelmaking where iron, steel scrap, and lime is processed at high temperature in Basic Oxygen (BOF) and Electric Arc (EAF) furnaces. Approximately 10-15% by weight of the output from the Basic oxygen furnace (BOF) is steel furnace slag or SFS. The source CW and SFS materials selected are Dendrobium coalwash from Illawarra Coal and a SFS produced via the basic oxygen method (BOS) by ASMS (Australia Steel Milling Services), respectively (Fig.17).

5.1.2 Field trial results

A field trial has been carried out at the Port Kembla Outer Harbor reclamation site, as shown in Fig. 18. The Port Kembla Port Corporation (PKPC) provided a 55m by 14m area for the field trial; the material in this area is 1.4m thick, which corresponds to a total volume of 1078m^3. The area is divided into two sections in order to assess the performance of two selected mixtures whose ratios are based on a preliminary study (Chiaro et al. 2013), i.e. CW50-SFS50 and CW20-SFS80 by volume percentage. These materials are mixed in an excavator and then spread and levelled in their designated area with a grader (Fig. 18). The blends of coalwash and steel furnace slags are compacted inside a 13-tonne smooth steel drum roller with a vibration mode at a frequency of 30Hz.

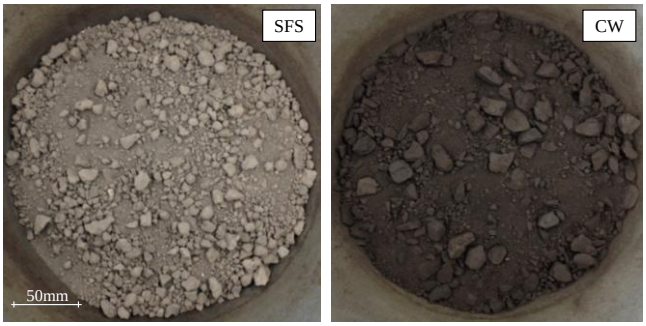

Figure 17. Typical aspect of steel furnace slag (SFS) and coal wash (CW) granular waste by-products

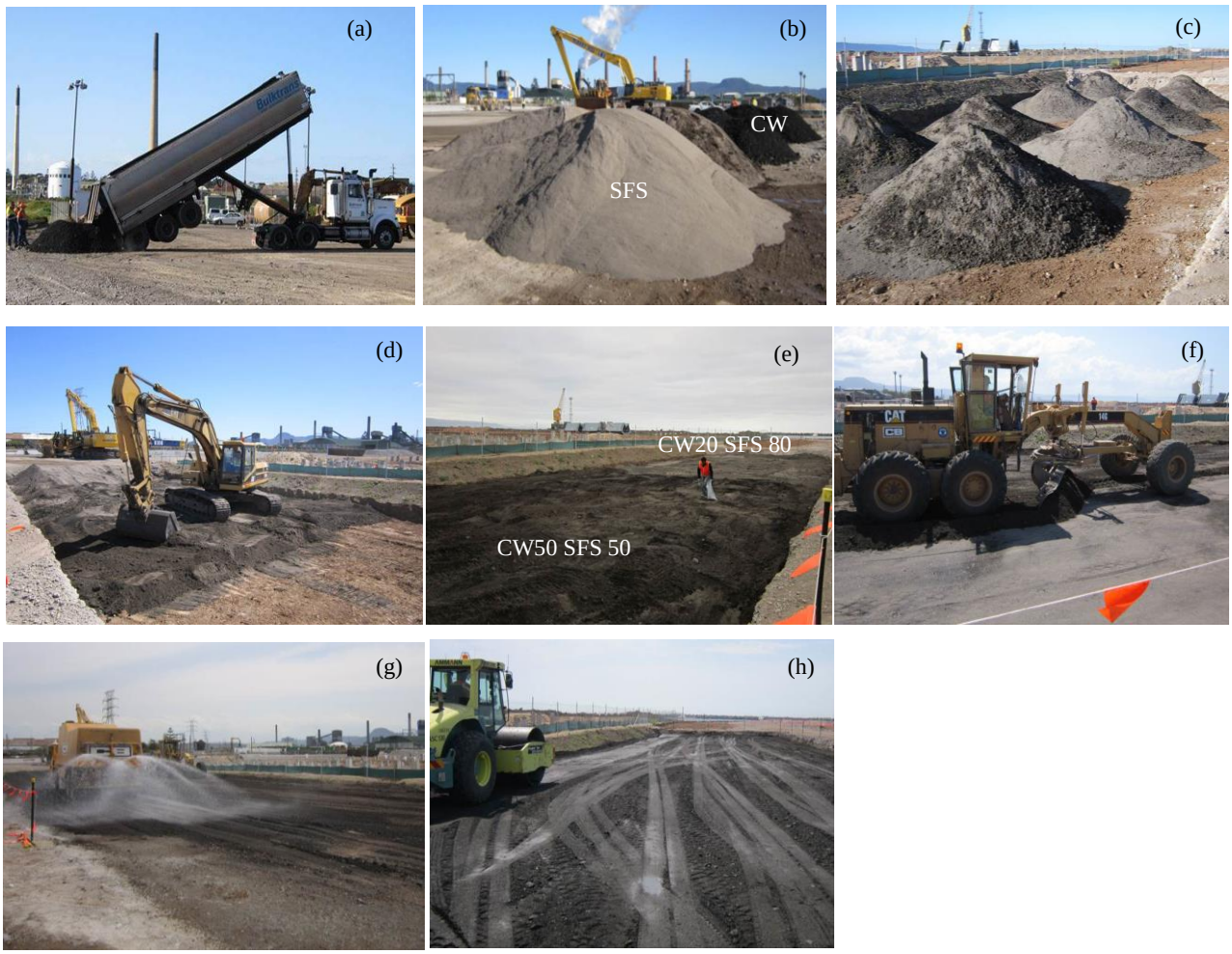

Figure 18. Photos of the field trial (a) arrival of the material on site, (b) stock pile of steel furnace slag and coalwash, (c) mixed materials ready for (d) spreading, (e) sampling prior to compaction, (f) levelling, (g) adding moisture and (h) compaction

To assess the post-compaction shear strength of the mixtures, Dynamic Cone Penetration Tests (DCPTs) and plate load tests (PLT) are carried out. In the DCPT tests the number of blows required to drive the cone penetrometer 100mm into the compacted layers is measured throughout the test, while the equivalent in-situ California Bearing Ratio (CBR) values are obtained via the number of DCPT blows ($CBR = 292/DCP^{1.12}$). Having equivalent CBR values between 25-50 means these mixtures are suitable for structural fill in terms of their shear strength. Each mixture is tested at two elapsed periods to investigate the hydration reactions taking place due to the free lime (CaO) and free magnesium (MgO) in the SFS. The variation of applied pressure with settlement at two stages (i.e. 30 and 170 days after compaction) is plotted in Fig. 20. As expected, the mixture with a higher percentage of steel furnace slag (Fig 20b) differs the most in the 30 and 170 day tests. A crust has formed on the surface, and thus a sitting pressure equal to 400kPa was identified in the results of the second stage. From a post-construction settlement viewpoint, under port service loads expected to range from 60-120kPa, the settlement would not exceed 1mm, which further confirms their suitability as structural fill.

The presence of free lime (CaO) and free magnesium (MgO) in the SFS may cause the mixtures to swell, so to investigate this potential (ratio of vertical expansion to the thickness of the layer) surface markers are monitored with time using surveying equipment. While the mixture with more SFS shows more swelling, it is still modest for a free swelling condition; the CW43-SFS57 and CW27-SFS73 are 6.3% and 5%, respectively. Furthermore, as long as the surcharge and live loads (e.g. pavement, live loads) exceed the swell pressure (approximately 50kPa for CW43-SFS57) no vertical expansion will occur. This indicates that if these mixtures are used in locations where the surcharge loads exceed 50kPa, which is almost equivalent to a typical pavement load (i.e. 30 - 45kPa); any potential swelling is unlikely to affect the performance and stability of the Port Infrastructure.

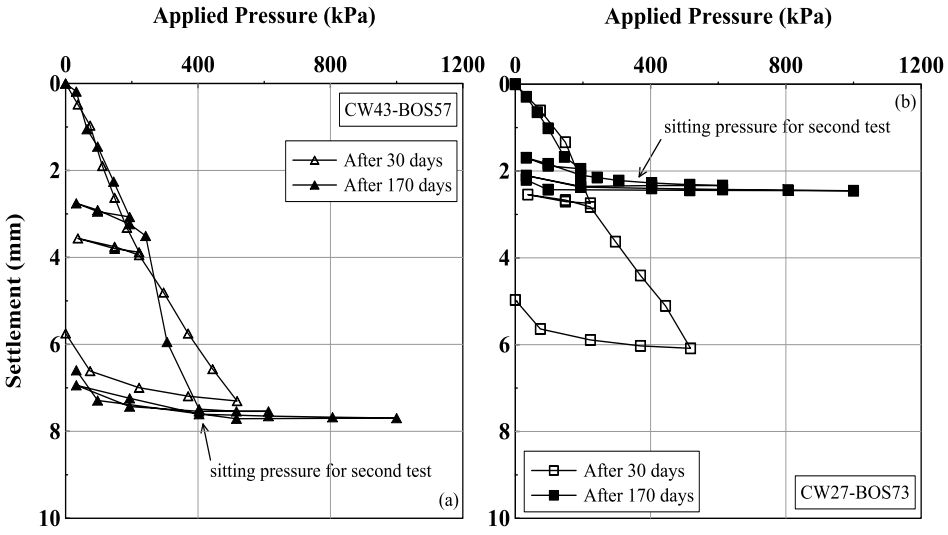

Figure 20. Variation of pressure against settlement on (a) CW43-BOS57 and (b) CW27-BOS73 (Tasalloti et al., 2015b)

5.2 CASE STUDY: PENRITH LAKES

The Penrith Lakes scheme, just north of Penrith, NSW covers over 2000 hectares. This site has operated as a quarry for many decades and has involved the removal of overburden, and sand and gravel to depths of 20m. The beginning of the Penrith lakes scheme in the early 80's involved removing sand and gravel and subsequent rehabilitation by backfilling the quarried areas. This filling work accords with the specifications on the Deed of Agreement (DOA), with placement and compaction using scrapers and compaction control based on certain relative maximum dry density (MDD) specifications. However, before this DOA, most of the landform had been carried out without any records of placement methodology, so these particular fill areas can be deemed as uncontrolled fill where the scope for future land use is restricted to parkland. This is why the current conditions in terms of its bearing capacity are extremely important. Preliminary field testing has been carried out in two smaller areas, DC Area 7 and 9, as shown in Figure 21. These areas serve as a benchmark to verify the methodology because they have been subjected to soil improvement by dynamic compaction (Figure 21), and subsequently assessed as satisfactory in terms of the bearing capacity needed to support the design requirements.

5.2.1 Post-compaction assessment

The backfilling material is a by-product of cobble quarrying activities widely used to fill low-lying areas at the Penrith Lakes (NSW, Australia). The soil consists of particles ranging from cobbles to silt/clay, and can therefore be classified as SP-SC (Unified Soil Classification System, USCS) and as A-2-4 (AASHTO method M145). The particles size distribution or PSD shows that the soil consists of 89% sand and 11% fines, of which 7% is silt and the remaining 4% is clay size particles. A model incorporating the combined use of matric suction and shear wave velocity (V_s) has been proposed to assess how well it is compacted. To evaluate the relationship between the compaction states (i.e. moisture content, dry unit weight, Figure 22), and the associated matric suction and V_s , a number specimens have been prepared. The shear wave velocity (V_s) propagation in the compacted specimens has been evaluated using Bender elements whereas the matric suction has been evaluated used a small tip tensiometer (ASTM D5298, 2003) and the filter paper method (ASTM D3404-91, 1998). Figure 22 shows the water retention data for specimens compacted at different energy levels.

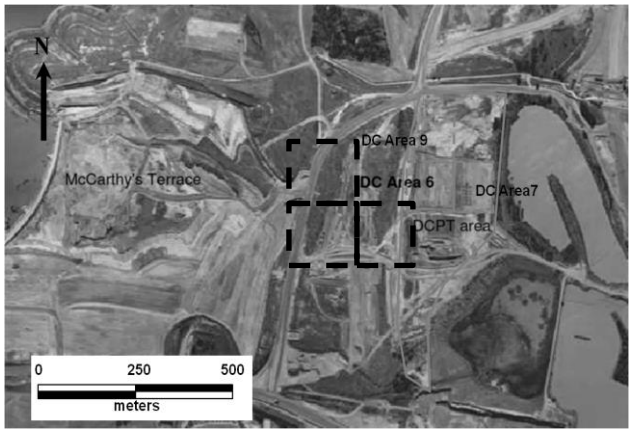

Figure 21: Location of benchmark areas 9 and 7 which encompass the Dynamic Compaction Prototype Trial (DCPT) area (modified after Heitor et al., 2015)

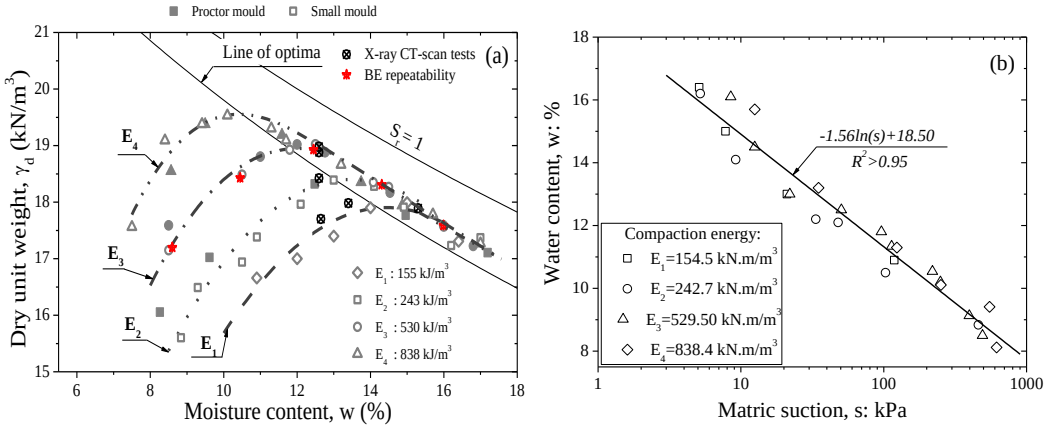

Figure 22: Compaction data (a) in terms of dry unit weight and water content and (b) matric suction (after Heitor et al., 2015)

Overall, the suction decreases as the water content increases, and although there is no apparent relationship between the suction and compaction energy, all the data points seem to converge to a logarithmic regression line. This suggests that the water content influencing the suction is more important than the compaction energy, and the field suction can be estimated once the moisture content is known. There is a good agreement between the predicted results and the actual trends (Figure 23).

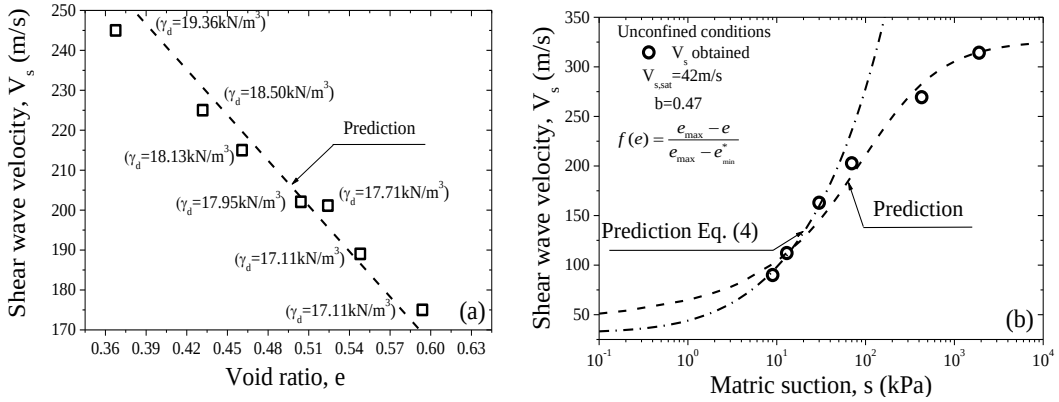

Figure 23: Comparison between the test data and model predictions, (a) influence of void ratio and (b) influence of suction (modified after Heitor et al., 2015)

5.2.2 Field Validation

To evaluate the current compaction conditions in terms of the dry unit weight of the fills, an empirical model that incorporates the field measurements of V_s and the suction, or water content, has been developed, and while the empirical model is assessed for laboratory tests, these tests occurred in laboratory controlled set-ups, which do not always represent field conditions, particularly in terms of material variability. The predictions regarding the reference soil calibration parameters and the field data for the selected borehole are shown in Figure 24, where overall, they match the field DHGD bulk density quite well, despite the anticipated variations in the ground material. There are strong discrepancies, particularly in the top 2m, which suggests that the initial estimate of 1.5m for the depth of influence H_s, based on the Thornthwaite moisture index (TMI) (Thornthwaite, 1948) may have been conservative because the prediction of bulk density to a depth of 2m is inaccurate.

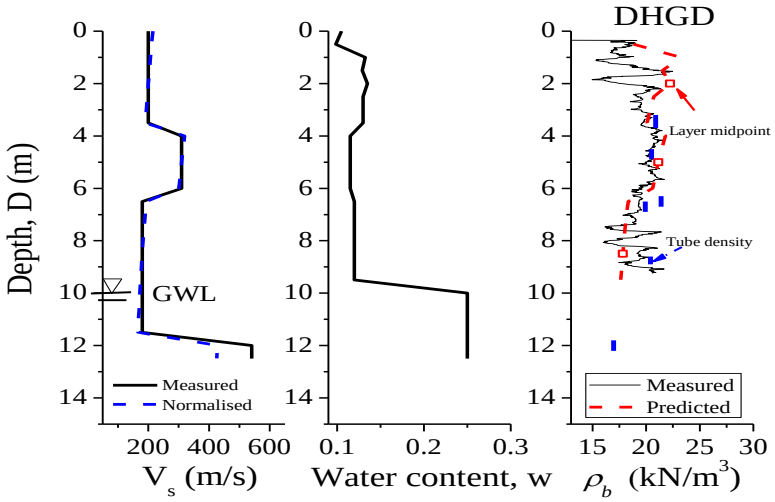

Figure 24: Comparison between the field measurements and model predictions

The graphical solution of the relationship proposed by Heitor et al, 2015, makes it possible to develop design charts to reference the relationship along the compaction plane. In Figure 25, the w-γ_d -Vs chart for a 100kPa level of field mean effective confining stress is plotted together with the standard compaction energy compaction curve and the degree of saturation lines of 1, 0.8, and 0.67. Note here that the equal Vs lines across the compaction are almost perpendicular to the degree of saturation lines; this is consistent with the experimental observations which show the close relationship between Vs and the degree of saturation (Heitor et al., 2013, Heitor et al., 2015).

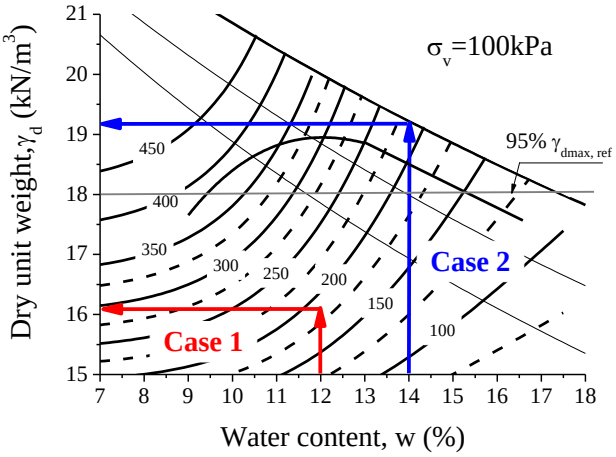

Figure 25: Illustration of the working flow of the w-γ_d -Vs quick reference charts

6 USE OF INFILLED WASTE TYRES FOR RAIL CAPPING

A numerical study has been used to investigate how rubber tyres confined in ballasted embankments affects its performance, with the analysis suggesting that infilled waste tyres can help reduce the vertical and lateral deformation of ballast embankments. These rubber tyres have a "mattressing" while the gravel composite could reduce the transmission of train loads to the subgrade underlying the substructure, both of which can provide higher bearing capacities and possibly less settlement while simultaneously helping to prevent lateral spreading.

6.1 FINITE ELEMENT ANALYSIS OF INFILLED WASTE TYRES FOR RAIL CAPPING LAYER

Table 2 summarises the material properties used in this analysis. The tyres are modelled as being cylindrical and there is no contact between them, as shown in Figure 26. By using symmetry, half of the embankment and foundation are modelled as shown in Figure 26. A series of simulations are carried out on the railway geometry to determine how the ballast affects the performance of the track, with and without rubber tyres. Each scenario is analysed with and without rubber tyres for comparison purposes.

Table 2: Finite Element material properties

Properties	Ballast	Rubber infilled gravel	Foundation	Rubber tyre	Rail	Sleeper
Mass Density, ρ (kg/m^3)	1530	1530	1700	1500	2000	2000
Elastic Modulus, E (MPa)	2	2	20	500	500000	30000
Poisson's Ratio, ν	0.3	0.3	0.35	0.35	0.3	0.25
Internal Angle of Friction (°), ϕ	45	45	--	--	--	--
Angle of Dilation (°), ψ	15	15	--	--	--	--

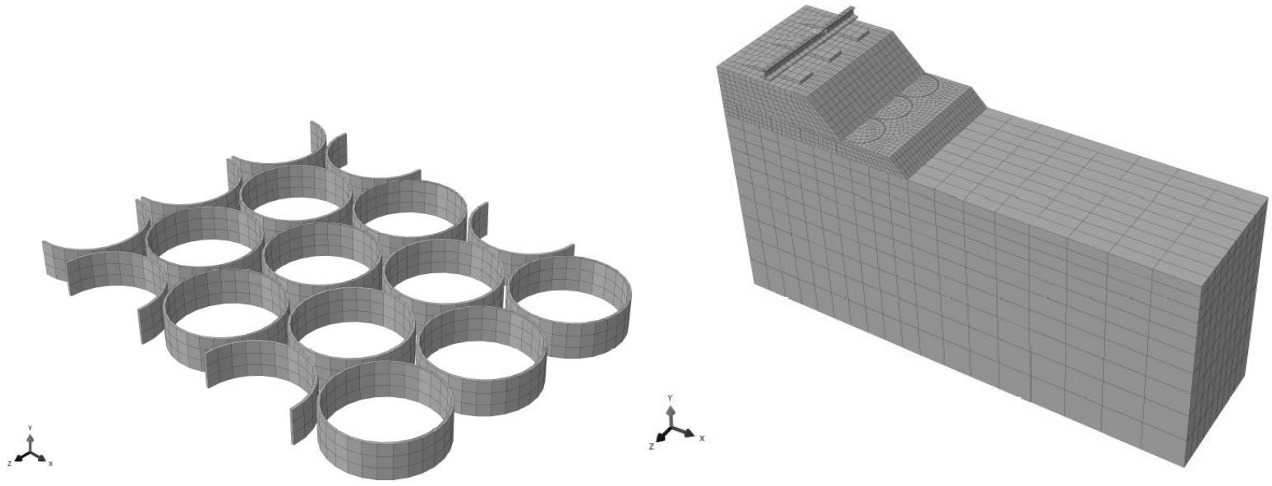

Figure 26: Mesh of embedded rubber tyres and ballasted railway track and foundation

Over many loading cycles, often measured in Millions of Gross Tons (MGT), ballast can deteriorate through abrasion and fracture due to asperities and faults. This "rounding" of particles and loss of resistance due to a reduction in angularity reduces the strength of ballast, and therefore it is relevant to see what benefits rubber tyres will provide to railway substructure, especially as it deteriorate, because it could be representative of old ballast or possibly demonstrating the potential of recycled ballast. To simulate the effects of confinement for a variety of materials with varying strengths, the internal friction angle of the ballast is simulated from 30° to 45°, to represent rounded to relatively fresh ballast. The subgrade stiffness is kept constant at 20 MPa (soft soil) throughout these simulations. The rubber tyres effectively reduced the vertical and lateral deformation of the ballast embankment, especially when low-quality material is used (Table 3). This result is very encouraging because ballast with a strength that is less than sub-standard could be used for the substructure, thus reducing the cost of construction. When gravel is low in strength (ϕ=30°), the use of rubber tyres help to reduce vertical settlement by almost 38%, from 123 mm of settlement to 77 mm of settlement below the sleeper (Table 3).

Table 3: Results of parametric study with varying ballast strength

Angle of internal friction (°)	Settlement under sleeper (cm)		Reduction (%)
	Rubber tyre	None	
30	7.69	12.33	37.63
35	6.36	9.07	29.38
40	5.41	7.37	26.59
45	4.91	6.28	21.82

As well as reducing the vertical deformation below the track structure, the rubber tyres also inhibit the substructure form spreading laterally along the slope of the ballasted foundation (Figure 27). As expected, the displacement in weaker materials is larger, but its magnitude decreases as the spreading decreases, by almost 51% (38 mm-77 mm) and 60% (102 mm-252 mm), for the ϕ=40° and ϕ=30° cases, respectively. Intuitively, this prevention of spreading will also reduce the vertical settlement, especially when ballast overlies a stiff foundation, because the substructure materials will not squeeze horizontally under heavy loads. As well as preventing displacement, confining rubber tyres will also increase the strength and stiffness of railroad substructure.

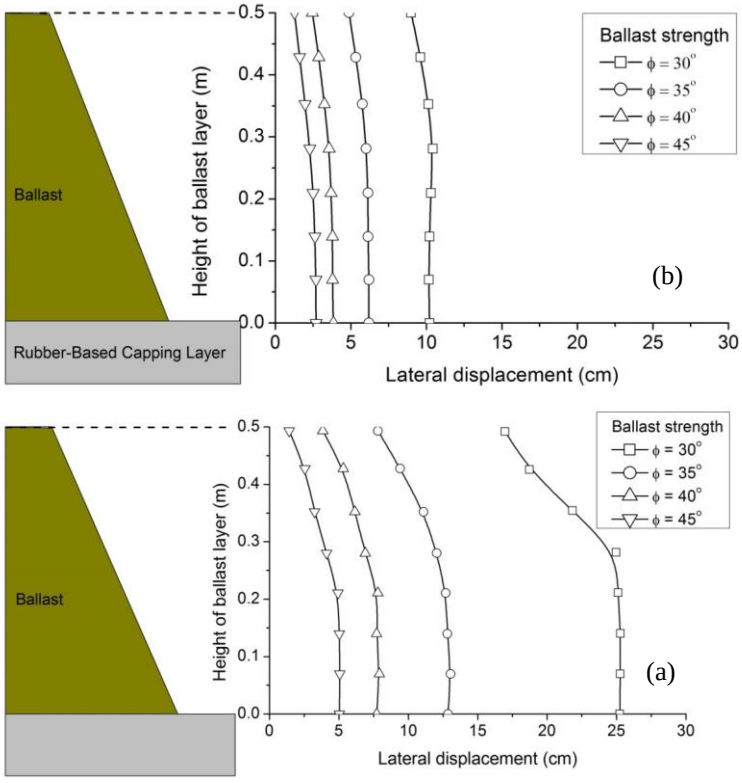

Figure 27 (a) Lateral displacement at slope of ballast layer with rubber tyres; (b) Lateral displacement at slope of ballast layer without rubber tyres

Another factor that preserves the structural integrity of ballast embankments is a reduction in the transmission of train loads to the subgrade underlying the substructure (Figure 28) due to the "matressing" effect of rubber tyres and the distribution of subgrade stress, as the analysis shows. In fact when rubber tyres are used with weaker ballast, there is a significant decrease in vertical stress on the subgrade, which reduces its peak by almost 18% (170-140 kPa) for ϕ=30° and 16% (155-130 kPa) for ϕ=35°, respectively.

7 USE OF SHOCK MATS FOR RAIL

The use of artificial shock mats such as Under Sleeper Pad (USP) and Under Ballast Mat (UBM) has become increasingly popular in recent years (Esveld 2001; Bolmsvik 2005; Marschnig and Veit 2011; Schneider et al. 2011) because they eliminate the hard interface with ballast and allow the aggregates to bed into the relatively softer pad, thus increasing the contact surface area between the ballast and the other interfaces; this then eliminates excessive contact

forces between the interfaces and ballast aggregates, and thus reduces settlement and breakage. Since the compression load is distributed over a larger contact area, it further reduces the force acting on the sleeper-ballast and ballast-base (hard subgrade) interface and mitigates excessive inter-particle contact forces in the ballast layer (Loy 2008; Dahlberg 2010).

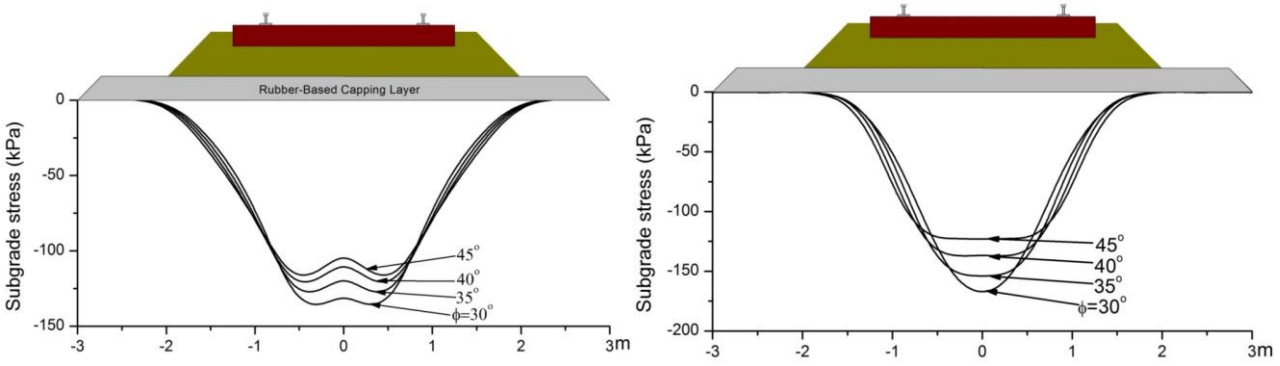

Figure 28: (a) Subgrade stress distribution below ballasted railway track with rubber tyres; (b) Subgrade stress distribution below ballasted railway track without rubber tyres

'Shock mats' in rail tracks can also attenuate the dynamic impact force and cyclic stresses. However, studies conducted to analyse how effectively they minimise ballast degradation are limited. Some of the research work undertaken using the state-of-the art large scale testing facilities at the University of Wollongong, and some relevant field studies carried out near Singleton, New South Wales (NSW), Australia are discussed in this section.

7.1 LARGE SCALE LABORATORY TESTING

To understand the role of shock mats in more detail, a series of cyclic and impact loading tests via the large-scale process simulation test chamber (Fig. 29a) at the University of Wollongong have been carried out by simulating the impact loads using the high-capacity drop-weight impact testing equipment (Fig. 29b). The fresh ballast is latite (volcanic) basalt, a common igneous rock that lies along the south coast of NSW, and obtained from Bombo quarry, near Wollongong. The subballast also came from Bombo quarry, NSW. These samples of ballast and subballast are prepared in accordance with current Australian practices (AS 2758.7, 1996).

Figure 29: (a) Process Simulation Test Apparatus; (b) High Capacity Drop Weight Impact Machine

7.2 CYCLIC LOAD TEST

Cyclic loading tests are carried out using a process simulation test chamber (Fig. 29a) which can 800 mm long by 600 mm wide by 600 mm high specimens. The bottom layer of the test sample is a 150 mm thick layer of compacted subballast overlain by 300 mm thick load bearing ballast. This ballast is placed and compacted in three equal layers by a rubber padded vibratory hammer to achieve a representative field density of 1560 kg/m^3. A rail-sleeper assembly is placed on top of the ballast and the space around the concrete sleeper is filled with 150 mm thick crib ballast. Two tests are carried out, one with USP and one without USP. The cyclic loading applied to the test sample is shown in Figure 30, and the total number of load cycles applied in each test is 500,000.

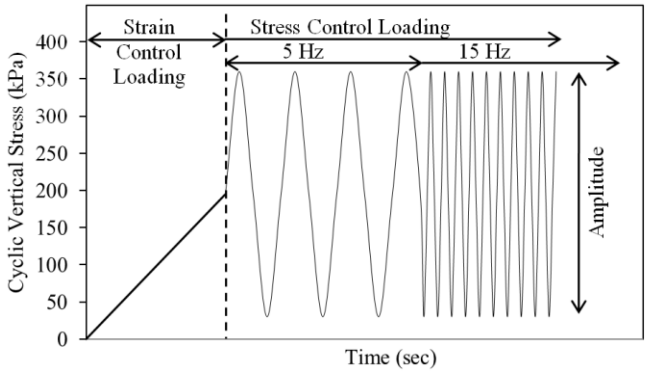

Simulated Axle Load	25 ton
Cyclic Loading Frequency	15 Hz
Simulated Train Speed	109 km/h
Maximum Cyc. Vertical Stress, $\sigma_{1max,cyc}$	360 kPa
Minimum Cyc. vertical Stress, $\sigma_{1min,cyc}$	30 kPa
Mean Cyc. Vertical Stress, $\sigma_{1mean,cyc}$	195 kPa
Amplitude, $\frac{1}{2}(\sigma_{1max,cyc}-\sigma_{1min,cyc})$	165 kPa

Figure 30: Applied Cyclic Loading

7.3 IMPACT LOADS

Wheel–rail impact forces occur throughout the life time of the track structure due to imperfections such as defects in the wheel and rail, and the location of welded joints. These types of impact loads are simulated using the high-capacity drop-weight impact testing equipment (Fig. 29b). Cylindrical ballast specimens 300 mm thick are prepared by being compacted in several layers inside a 7 mm thick membrane with a rubber padded hammer, to meet a typical field density of 1560 kg/m^3. Two types of subgrade conditions are simulated; a typical weak subgrade condition using a 100 mm thick sand layer vibro-compacted to a density of 1620 kg/m^3, and a hard subgrade simulated by a 50 mm thick rigid steel plate to resemble bridges and bedrock.

The test specimens are placed on the concrete floor and aligned with the drop hammer. Typical dynamic stresses between 400-600 kPa caused by wheel flats and dipped rail (Jenkins et al. 1974; Indraratna et al. 2010) are simulated by the drop hammer. This impact loading is repeated 10 times per sample because the ballast strains are attenuated after 8 or 9 impact blows. Data are collected at a frequency of 50,000 Hz.

7.4 SHOCK MATS

Two types of shock mats are used in this study. The 10 mm thick elastoplastic USP for testing the cyclic load is made from polyurethane and is glued to the bottom of the concrete sleeper. The recycled rubber shock mats used for impact load testing are 10 mm thick, and are made from recycled rubber granulates encapsulated within a polyurethane elastomer compound. These shock mats are used in 3 layers with an overall thickness of 30 mm, and are placed at either the top or the bottom of the ballast layer. The mechanical properties of the shock mats are shown in Table 4. USP mats are generally stiffer than UBM mats because they are placed adjacent to higher stress zones, i.e., sleeper-ballast interface, however, to evaluate their relative efficiency under impact, the same thickness and type of material is used for the USP and UBM mats (Table 4; right hand columns).

Table 4: Mechanical Properties of Shock Mats

Shock Mat (USP) for Cyclic Load Test		**Shock Mat (USP & UBM) for Impact Load Test**	
Thickness	10 mm	Thickness	10 mm
Weight	4.2 kg/m^2	Young's Modulus	6.12 MPa
Bedding Modulus	0.22 N/mm^3	Tensile Strength	600 kPa
Average Tear Strength at USP-Sleeper	0.5 MPa	Tensile Strain at Failure	80%

7.5 FIELD INVESTIGATION

Ballast degradation is usually severe under stiff subgrade conditions, and the accelerated degradation of track geometry in these localised areas can increase the costs to railroads due to maintenance, speed restrictions, and stoppage and delays. Moreover, failures of the track and vehicle components, damage to bridge structures and mud pumping from fouled ballast are more common at these places. To investigate their effectiveness, shock mats were placed at the Mudies Creek bridge at Singleton, NSW. Figure 31 shows the location of the test bridge and installation of the shock mats. A layer of UBM was installed underneath the ballast layer, on top of the concrete bridge deck.

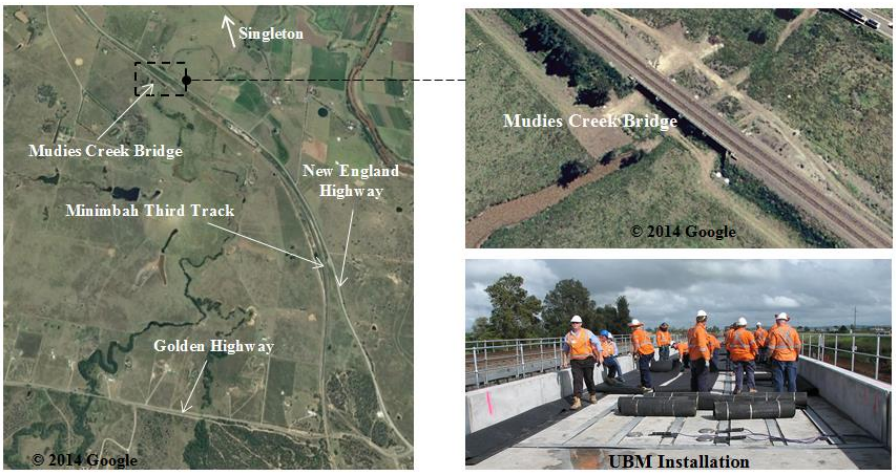

Figure 31: Mudies Creek Bridge Location and Installation of UBM (sourced from Indraratna et al. (2014))

7.6 RESPONSE TO CYCLIC AND IMPACT LOAD STRAINS

The shear and volumetric strains of e ballast under cyclic loading with and without USP are calculated from the vertical and lateral displacement of ballast measured at a certain number of load cycles (e.g. N = 100, 500, 1000, 5000, 10000, etc.). The shear (ε_q) and volumetric (ε_p) strains with and without the USP are shown in Figure 32 (a) and (b), respectively. Strain in the ballast up to around 10,000 cycles is rapid due to its initial densification and further packing after corner breakage of the sharp angular aggregates, but once the ballast became stable after 10,000 cycles, the rate of strain decreases as the load cycles increase. When USP is used, the shear and volumetric strains decreased between 25 to 30% for the same applied cyclic load and frequency.

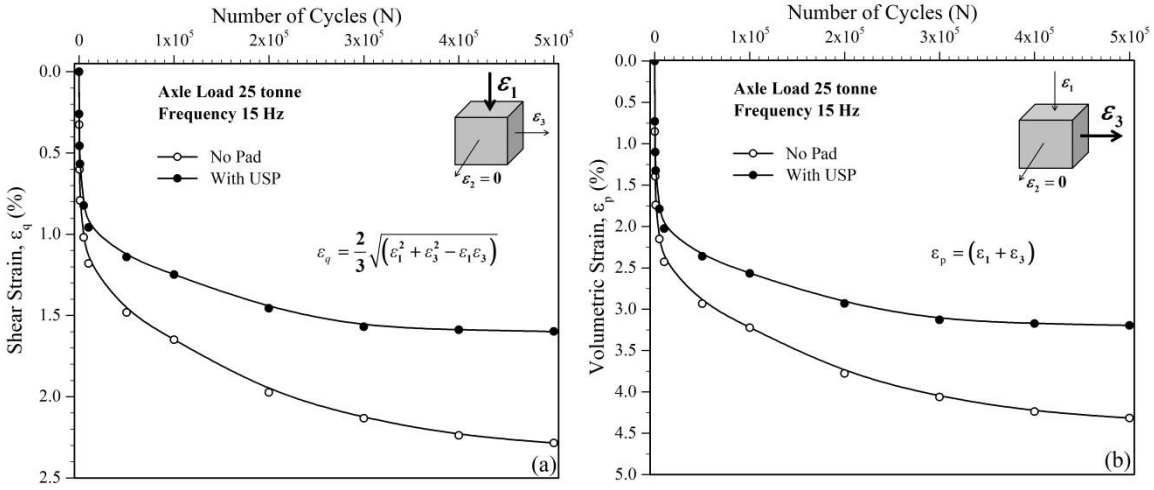

Figure 32: Cyclic strain of ballast with and without shock mats,
(a) Shear strain; (b) Volumetric strain (data sourced from Indraratna et al. (2014))

The variation of shear and volumetric strains with and without shock mats for the soft and hard subgrades under impact laods is shown in Figure 33(a) and (b), respectively. The shear and volumetric strains are both higher for ballast without shock mat, and decreased between 40 - 50% when the shock mats are introduced at the top or bottom of the ballast layer. The strains increase rapidly with the initial impact blows but then stabilise after almost 8 impact blows. This is

due to the rearrangment and corner breakge of ballast particles at the initial stage of loading and gradually diminishing thereafter. The strain values are more pronounced for hard subgrade than the soft subgrade.

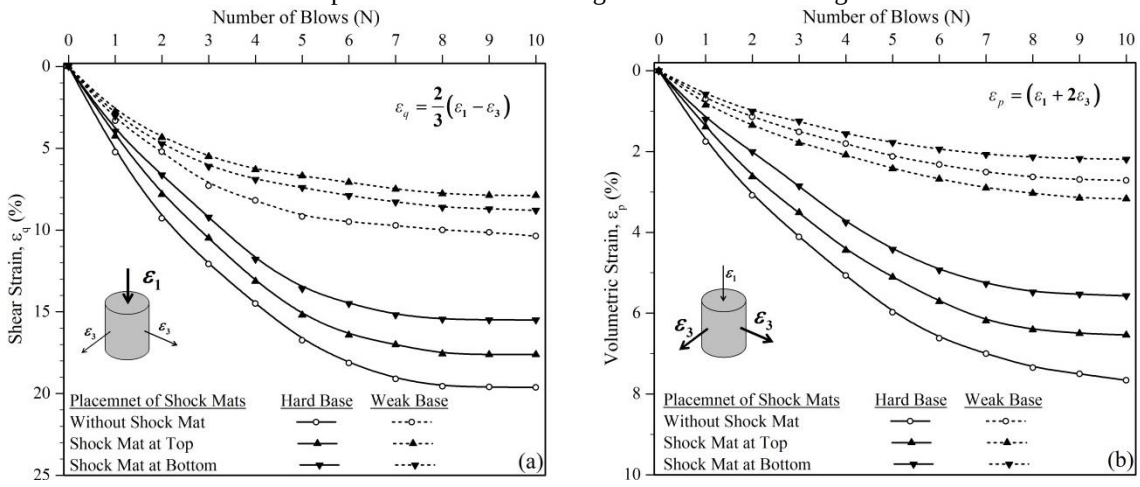

Figure 33: Impact Strain Response of ballast with and without shock mats
Shear strain; (b) Volumetric strain (data sourced from Nimbalkar et al. (2012))

7.7 BALLAST DEGRADATION

The particle breakage due to cyclic and impact loading is assessed by using the parameter and Ballast Breakage Index (BBI) proposed by Indraratna et al. (2005). In order to estimate ballast breakage better, the ballast layer is divided into three layers of equal thickness, and then the BBI values are assessed separately for the top, middle, and bottom layers. Representative samples of ballast have been collected at the Mudies Creek Bridge site to estimate particle breakage. Three equal portions of load-bearing ballast are sampled beneath the sleeper at the rail seat after about 8×10^5 load cycles. The calculated BBI for each layer under cyclic and impact loads are presented in Table 5 for conditions with and without shock mat. The table also present the results of BBI for the sample collected at the bridge site.

It is evident that the ballast breakage was significantly lessened by the use of USP under cyclic loading. The ballast breakage is higher at the top layer as expected due to the higher inter-particle contact stress at the top, followed by the middle and bottom layers. In impact load test, the ballast breakage was significantly reduced by the shock mats, and the degradation is more pronounced for a hard subgrade than for a soft subgrade. Based on the field study, the ballast breakage decreased with depth of the ballast layer when shock mat placed above the bridge deck.

Table 5: Ballast Breakage Index (BBI)

BBI Estimated at	Cyclic Load Test		Impact Load Test						Field Data
			Hard Base			Weak Base			
	Without Shock Mat	With USP	Without Shock Mat	With USP	With UBM	Without Shock Mat	With USP	With UBM	With UBM
Top Layer	0.071	0.026	0.131	0.104	0.122	0.069	0.042	0.061	0.026
Middle Layer	0.056	0.023	0.099	0.075	0.085	0.048	0.035	0.041	0.023
Bottom Layer	0.053	0.020	0.280	0.257	0.181	0.123	0.090	0.066	0.020

8 NATIVE VEGETATION FOR TRANSPORT CORRIDORS

While bioengineering applications in civil engineering using begin with slope stabilisation and erosion control, the vegetation used can also influence the soil water balance and hydrogeology of the site. A railway line is an engineering structure which is greatly influenced by hydrological and environmental conditions, and given the lengthy rail networks in coastal areas of Australia, many rail tracks are built on clayey soils that are sensitive to moisture, which is why

bioengineering methods for improving the ground are becoming increasingly popular means for stabilising railway corridors.

Tree roots provide three stabilising functions: (a) they reinforce the soil, (b) they dissipate excess pore pressure, and (c) they help to establish sufficient matric suction to increase the shear strength. The studies presently available indicate that most attempts to quantify the effects of vegetation only focus on the structural reinforcement provided by roots, whereas very few attempts are made to relate the changes in soil strength and stiffness to the rate of transpiration.

Despite these advantages, geotechnical engineers are reluctant to adopt vegetation-based stabilisation partly because vegetation is perceived to be unpredictable and therefore non-uniform patterns of soil moisture reduction may develop, and also because they are time dependent. Moreover, Biddle (1998) and McInnes (1986) reported the detrimental effect that vegetation has on buildings and pavements, whereas new field observations indicate that where there are trees beside railway tracks, their localised, undrained failure is minimal. In reality the use of native vegetation in remote railway lines in Australia to stabilise existing railway corridors built over expansive clays and compressive soft soils is beneficial because properly selected and used vegetation such as native trees and shrubs can reduce soil moisture by root water uptake and also increase its shear strength and stiffness by increasing the matric suction and controlling erosion.

An analytical model based on the root water uptake (Indraratna et al., 2006) as a function of potential transpiration, root density and suction reduction factor has been developed to predict the suction existing around tree roots.

8.1 CASE STUDY: MIRIAM SITE

The proposed site is at Miram village (Kaniva, Victoria) where the Eucalyptus largiflorens tree is monitored. According to Lawrence (1975), the oldest surficial unit is Tertiary Plicoene marginal marine Parilla sand, where the cross sections show a tertiary sequence between 100 to 330m thick (Figure 34). The climate in Miram is semi-arid with mild winters and long hot summers. The mean daily maximum temperature ranges from 13.7°C in July to 29.7°C in January. The mean monthly rainfall ranges from 20.9 mm in January to 47.7 mm in August, with a mean annual rainfall of 415.3 mm. The mean monthly potential evaporation ranges from 30.45 mm in July to 257.9 mm in January (Bureau of Meteorology, 2006). On an annual basis, the potential evaporation (1483.7 mm/yr) is more than 3 times the average annual rainfall (415.3 mm/yr).

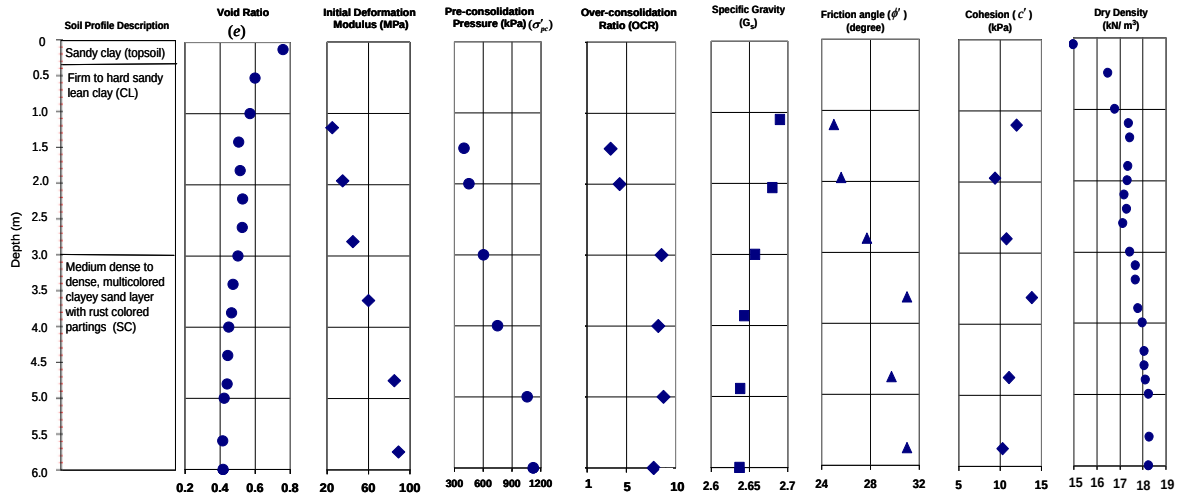

Figure 34 Profiles of soil properties at Miram site, VIC, Australia (modified after Fatahi et al. 2014)

The profile of average matric suction measured near a tree in the middle of May 2005 is shown in Figure 35. The field measurements indicate that the minimum moisture content and maximum matric suction of the top 3m soil are 9% and 1700 kPa, respectively, and therefore the soil wilting point suction ψ_w is estimated to be around 1700 kPa. The parameters used in this analysis relating to the interaction between the tree and the atmosphere are given in Table 6.

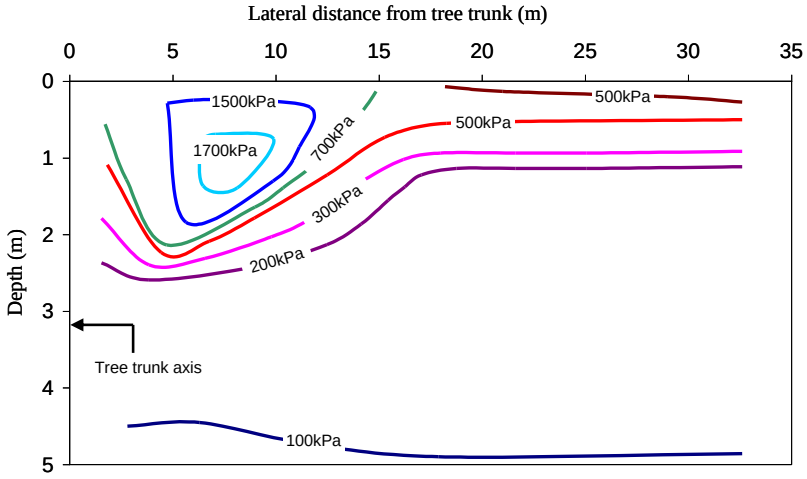

Figure 35 Profile of the distribution of average matric suction near eucalyptus largiflorens tree

Table 6: Parameters of interaction between tree and ground of a Black Box tree at Miram

Parameter	Measured Value	Comments
T_p	80 l/day	Estimated from Slavich et al. (1998) and Jolly and Walker (1996)
ψ_w	1700 kPa	Estimated from field measurements
ψ_{an}	4.9kPa	Clayey soil with air content of 0.04 (Feddes et al. 1976)
r_{max}	20m	Estimated from field observation
z_{max}	3m	Estimated from field observations
r_0	8.5m	Radial coordinate of the maximum root density point
z_0	1.2m	Vertical coordinate of the maximum root density point
$\beta_{f\cdot max}$	659000 m^{-2}	Measured according to organic content
k_1	0.35	Measured according to organic content
k_2	0.55	Measured according to organic content

A two dimensional finite element analysis is used to predict the distribution of the soil moisture content and matric suction near the tree (Figure 36). The numerical analysis in this case study is based on the basic effective stress theory of unsaturated soils incorporated in the ABAQUS finite element code. The axi-symmetric model and specified boundary conditions are shown in Figure 36.

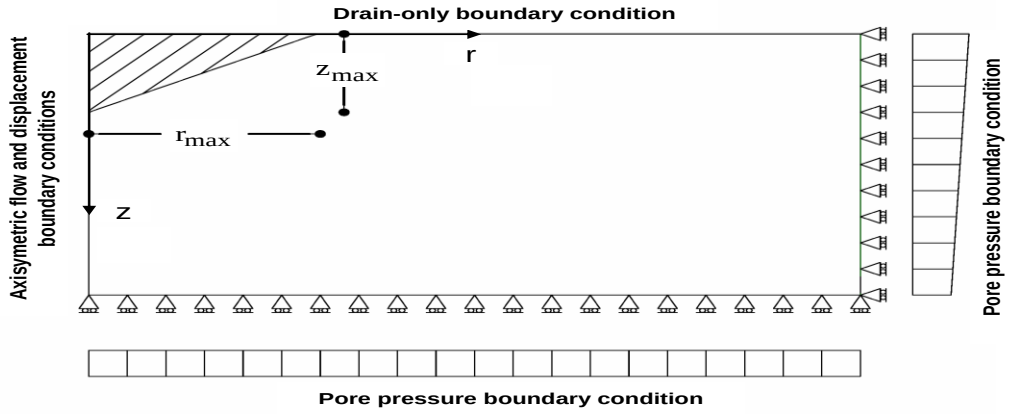

Figure 36: Geometry and boundary conditions of the model

The mesh used in this simulation contains axi-symmetric, bi-linear strain quadrilateral elements (CAX4P) with 4 displacements and pore pressure nodes at the corners of each element. The entire FE mesh consists of 3,993 nodes and 3,840 elements. The flux boundary at the surface is controlled by climatic conditions such as the rainfall and

evaporation rates. It is assumed in this study that other hydrological features such as irrigation, surface runoff, and surface storage are negligible. Evaporation and rainfall rates have been applied at the surface on a daily basis using the non-uniform distributed flow that represents the magnitude of the flow rate on the surface. The model used in this study to estimate the actual evaporation rate as a function of potential evaporation is based on the approach originally proposed by Aydin (1998) where it is assumed that any initial evaporation from a saturated soil proceeds at the potential rate until air entry suction is reached at the soil surface. When the air entry suction value is reached, evaporation in the soil begins to drop, in fact, beyond the value of the air entry suction, evaporation continues to fall and the surface becomes progressively drier until it reaches wilting point suction. When this point is reached, the amount of evaporation is insignificant. According to Aydin et al. (2005), the ratio of actual to potential evaporation can be linearly correlated to the log-transformed soil matric suction. However, although the soil water evaporates slowly when it is beyond the wilting point suction, water is still lost through the slow process of vapour diffusion. In this study it is assumed that any water lost by vapour diffusion is negligible.

Figure 37 shows a comparison between the field measurements and predictions made by the numerical model for the volumetric moisture content. The numerical results which incorporate the developed root water uptake model basically agree with the field measurements, although the field measurements for the moisture content reduction are noticeably different from the finite element predictions close to the tree trunk. This is not surprising because the trunk and its foliage alters the uniform distribution of rainfall, and the shadow under the canopy changes the rate of evaporation due to variations in temperature and humidity. As a consequence, these effects probably caused the disparity between the field data and finite element predictions.

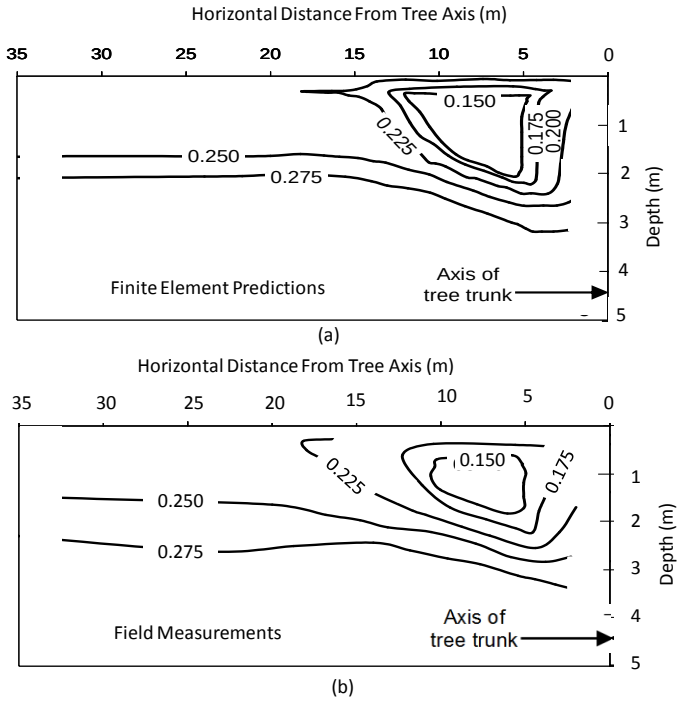

Figure 37: Contours of volumetric soil moisture content reduction in vicinity of the tree (a) current numerical analysis results, (b) field measurements (modified after Fatahi et al. 2014)

9 CONCLUSIONS

The 'field' performance of ballasted rail tracks with geosynthetic reinforcement has been discussed and the performance of instrumented ballasted tracks at Bulli and Singleton using different types of ballast and geosynthetic reinforcements has been evaluated. This Bulli study indicates that using geocomposite to reinforce recycled ballasted tracks is a feasible and effective alternative, whereas the Singleton indicates that geosynthetics became more effects as the stiffness of subgrade decreases. The strains that accumulate in geogrids are influenced by the deformation of the subgrade whereas the induced transient strains are mainly affected by the stiffness of geogrids however, a better understanding of this performance would enable a safer and more effective design and analysis of ballasted rail tracks with geosynthetic reinforcement.

The finite element analysis of track behaviour prior to track construction is considered to be a Class A prediction with real time field monitoring since construction commenced. Here the PVDs reduce the build-up of excess pore water pressure (EPWP) during cyclic loading quite significantly, and continued to dissipate it during the rest period; this dissipation of EPWP during the rest period makes the track more stable for the next loading stage. Even with relatively

short PVDs, the predictions and field data prove that lateral displacement can be curtailed, and the equivalent plane strain finite element analysis is well able to predict the behaviour of track improved by short PVDs.

At the 45 ha reclamation project at the Outer Harbour extension of Port Kembla in Wollongong, the potential use of CW and SFS as the predominant reclamation fill as an alternative to conventional freshly quarried or dredged sand fills has been examined. Detailed laboratory investigations indicate there is an optimum CW-SFS mixture that would meet most of the geotechnical specifications needed for it be used as an effective structural fill. To evaluate the in situ behaviour of CW-SFS mixtures (50% CW + 50% SFS and 20% CW + 80%) and determine the most suitable compaction methodology and associated machinery, the field trial tests delivered encouraging outcomes.

The numerical study investigating the effects of confining rubber tyres in ballasted embankments suggests that infilled waste tyres will definitely reduce its overall deformation because the "mattressing" effect of rubber tyres and gravel composite reduces the transmission of train loads to the subgrade formation, which then provides higher bearing capacities and the possibility of less settlement.

An analytical model based on the root water uptake as a function of potential transpiration, root density, and suction reduction factor enables the suction around tree roots to be predicted. Moreover, the proper use of vegetation such as native trees and shrubs can reduce soil moisture by root water uptake and also increase its shear strength and stiffness by increasing the matric suction and controlling erosion.

Improving soft ground by installing stone columns increases its bearing capacity and accelerates the consolidation of transport embankments. This study shows that the stress concentration ratio depends on the time, depth, and PSD, while clogging retards the overall consolidation process. The degree of improvement in the strength and stiffness of soil is affected quite significantly by the column geometry, ground condition, and loading pattern. Column lateral deformation varies with depth and time, while the build -up of pore water pressure due to cyclic loading progressively increases with the number of cycles, but this rise depends on the loading frequency, and the amplitude and initial consolidation. Stone columns can be used to mitigate the build- up of cyclic excess pore pressure.

The experimental data confirmed that when assessing the current conditions of compaction fills, the use of shear wave velocity alone is not enough because Vs remained approximately constant across the dry side of the compaction plane. Moreover, a field evaluation of suction would be limited to the measuring capacity (i.e. 100kPa) of the available instruments, so it is better to determine the moisture content in the field. These field tests evaluated the in situ Vs using the MASW method and moisture content using density tube tests. The results indicate that the tested ground satisfies more than 95% of the relative compaction criteria initially anticipated, given that the area has already been treated by dynamic compaction. This methodology, unlike conventional geotechnical surveys, offers a valuable alternative in terms of cost and time savings.

10 ACKNOWLEDGEMENTS

The Authors wish to thank the Australian Research Council, NSW EPA's Waste Less, Recycle More initiative , CRC for Rail Innovation, Sydney Trains (formerly, RailCorp), ARTC, ARUP, Penrith Lake Development Corporation, Coffey Geotechnics, Queensland Rail National, Douglas Partners, Port Kembla Port Corporation, Queensland Transport & Main Roads, Menard Bachy, Indian National Jute Board, GHD, City of Salisbury Council, Transports for NSW (formerly NSW Transport Construction Authority), Tyre Stewardship Australia, BHP Billiton and Ecoflex International for their continuous support. The assistance of David Christie (formerly Senior Geotechnical Consultant, Rail Infrastructure Corporation (NSW)), Tim Neville (ARTC), Michael Martin (QR National), Geoff McIntosh (Douglas Partners), Dr Richard Kelly (SMEC), Mr Nathan Narendranathan (Infratech, Perth) and Dr Michael Biabani (Coffey) is gratefully acknowledged. The advice and help over a long period of time by Professors Harry Poulos (Coffey) and AS Balasubramaniam, Griffith University (Qld) is appreciated. A number of current and past doctoral students, including Dr Joanne Lackenby, Dr Wadud Salim, Dr Iyathurai Sathananthan, Dr Ali Tasalloti and current and past University of Wollongong colleagues, Dr Trung Ngo, Dr Qideng Sun, Dr Sudip Basak and Dr Sanjay Nimbalkar have all contributed to the contents of this paper. A significant portion of these contents have been reproduced with kind permission from the Journal of Geotechnical and Geoenvironmental Engineering ASCE, Geotechnique, and Canadian Geotechnical Journal, ICE Ground Improvement.

11 REFERENCES

Aydin, M. (1998). *Hydraulic properties and water balance of a clay soil cropped with cot-ton.* Irrigation Science, 15, 17-23.

Aydin, M., Yang, S. L., Kurt, N., and Yano, T. (2005). "Test of a simple model for estimat-ing evaporation from bare soils in different environments." Ecological Modelling, 182, 91–105.

Basack, S., Indraratna, B., Rujikiatkamjorn, C. and Siahaan, F. (2015a). *Theoretical and numerical perspectives on performance of stone column improved soft ground with reference to transport infrastructure.* In: Indraratna,

B., Jian, C. and Rujikiatkamjorn, C. (eds.).Ground Improvement: Case Studies, Elsevier Geo-Engineering Book Series, 1, 751-795.

Basack, S., Indraratna, B. and Rujikiatkamjorn, C. (2015b). *Modelling the performance of stone column reinforced soft ground under static and cyclic loads.* J. Geotech. Geoenviron. Eng., 142(2), 04015067-1- 04015067-15.

Bergado, D.T., Teerawattanasuk, C. (2008) *2D and 3D numerical simulations of reinforced embankments on soft ground*. Geotextiles and Geomembranes, Volume 26, pp 39-55,.

Biabani, M. M., N.T. Ngo and Indraratna. B (2016) *Performance evaluation of railway subballast stabilised with geocell based on pull-out testing.* Geotextiles and Geomembranes 44(4): 579-591.

Biddle, P. G. (1998). *Tree Root Damage to Buildings*, Willowmead Publishing Ltd., Wantage.

Bolmsvik, R. (2005). Influence of USP on track response–a literature survey. Abetong Teknik ABVäxjö, Sweden.

Chiaro, G., Indraratna, B., Tasalloti, S. M. A. & Rujikiatkamjorn, C. (2014). Optimisation of coal wash-slag blend as a structural fill. Ground Improvement, DOI: 10.1680/grim.13.00050 (in press, available online).

Dahlberg, T. (2010). *Railway Track Stiffness Variations - Consequences and Countermeasures.* International Journal of Civil Engineering, 8(1), 1-12.

Esveld, C. (2001). Modern railway track, MRT-Production, The Netherlands.

Fatahi, B., Khabbaz, H. & Indraratna, B. (2009). *Parametric studies on bioengineering effects of tree root-based suction on ground behavior*, Ecological Engineering, v35(10), 1415-1426.

Fatahi, B., Khabbaz, H. & Indraratna, B. (2010). *Bioengineering ground improvement considering root water uptake model*, Ecological Engineering, 36(2), 222-229.

Fatahi, B., Khabbaz, H. & Indraratna, B. (2014). *Modelling of unsaturated ground behaviour influenced by vegetation transpiration*, Geomechanics and Geoengineering: An International Journal, 9(3), 187-207.

Heitor, A., Indraratna, B. and Rujikiatkamjorn, C. (2013). *Laboratory study of small-strain behavior of a compacted silty sand*. Canadian Geotechnical Journal 50(2): 179-188.

Heitor, A., Indraratna, B., Rujikiatkamjorn, C., Chiaro, G. and Tasalloti, S.M.A. (2015)"Evaluation of the coal wash and steel furnace slag blends as effective reclamation fill for port expansion, In Proc. of the 7th International Congress on Environmental Geotechnics, A. Bouazza, S. T. S. Yuen, & B. Brown, (Eds.), 10-14 November 2014, Melbourne, Australia, 972-979.

Heitor, A., Indraratna, B., Rujikiatkamjorn, C., Golaszewski, R. (2015) *Assessment of the post-compaction fill characteristics at Penrith Lakes Development site*, in Ground Improvement – Case Histories edited by Indraratna, B., Chu, J. and Rujikiatkamjorn, C., Elsevier, 399 - 429.

Heitor, A., Indraratna, B. and Rujikiatkamjorn, C. (2015) The role of compaction energy on the small strain properties of a compacted silty sand subjected to drying-wetting cycles Géotechnique. Vol. 65 (9), pp. 717-727 (DOI: http://dx.doi.org/10.1680/geot.14.P.053)

Hird, C.C., Pyrah, I. C., and Russell, D. (1992) *Finite element modelling of vertical drains beneath embankments on soft ground*. Geotechnique, Volume 42, pp 3, 499–511,.

Indraratna, B. (1994). *Geotechnical Characterization of Blended Coal Tailings for Construction and Rehabilitation Work*. Quarterly Journal of Engineering Geology and Hydrogeology, 27, 353-361.

Indraratna, B., and Redana, I. W. (2000) *Numerical modeling of vertical drains with smear and well resistance installed in soft clay*. Canadian Geotechnical Journal, Volume 37, pp 132-145.

Indraratna, B., Rujikiatkamjorn C., and Sathananthan, I. (2005a) *Analytical and numerical solutions for a single vertical drain including the effects of vacuum preloading*. Canadian Geotechnical Journal, Volume 42, pp 994-1014.

Indraratna, B., Sathananthan, I., Rujikiatkamjorn C. and Balasubramaniam, A. S. (2005b) *Analytical and numerical modelling of soft soil stabilized by PVD incorporating vacuum preloading*. International Journal of Geomechanics, ASCE, Volume 5, pp 114-124.

Indraratna, B., Lackenby, J., and Christie, D. (2005). *Effect of confining pressure on the degradation of ballast under cyclic loading.* Géotechnique, 55(4), 325-328.

Indraratna, B., B. Fatahi and H. Khabbaz (2006). *Numerical analysis of matric suction effects of tree roots.* Proceedings of the Institution of Civil Engineers: Geotechnical Engineering 159(2): 77-90.

Indraratna, B., Attya, A., and Rujikiatkamjorn, C. (2009a) *Experimental investigation on effectiveness of a vertical drain under cyclic loads*. Journal of Geotechnical and Geoenvironmental Engineering, ASCE, Volume 135: 835-839.

Indraratna, B., and Rujikiatkamjorn, C., Kelly, R., and Buys, H. (2009b) *Soft soil foundation improved by vacuum and surcharge preloading at Ballina Bypass, Australia*. International Symposium on Ground Improvement Technologies and Case Histories (ISGI09): 95-105.

Indraratna B, Basack S, Rujikiatkamjorn C (2013). *Numerical Solution to Stone Column Reinforced Soft Ground considering Arching, Clogging and Smear Effects*. J. Geotech. Geoenv. Engrg., 139 (3), 377-394.

Indraratna B, Siahaan F, Rujikiatkamjorn C (2014). Three Dimensional Modeling of Stone Column Behavior using the Discrete Element Method. Proc. Micro to Macro, University of Cambridge.

Indraratna, B., Heitor, A., Rujikiatkamjorn, C. (2015) Ground improvement methods for port infrastructure expansion. Geotechnical Engineering, Journal of the SEAGS & AGSSEA 46 (3), pp. 125-130.

Jamiolkowski, M., Lancellotta, R., and Wolski, W. (1983) *Precompression and speeding up consolidation*. Proc. 8th ECSMFE: 1201-1206,.

Jenkins, H. M., Stephenson, J. E., Clayton, G. A., Moorland, J. W., and Lyon, D. (1974). "The effect of track and vehicle parameters on wheel/rail vertical dynamic forces." Railway Engineering Journal, 3(1), 2-16.

Leventhal, A. R. and de Ambrosis, L. P. (1985). *Waste disposal in coal mining—a geotechnical analysis.* Engineering Geology 22(1): 83-96.

Loy, H. (2008). "Under Sleeper Pads: improving track quality while reducing operational costs." European Railway Review, Russell Publishing, Kent, UK.

Richart F.E. (1957). *A review of the theories for sand drains*. Journal of the Soil Mechanics and Foundations Division, ASCE, Volume 83, pp 1-38,.

Rujikiatkamjorn, C., Indraratna, B. & Chiaro, G. (2013). *Compaction of coal wash to optimise its utilisation as water-front reclamation fill.* Geomechanics and Geoengineering, 8, 36-45.

Selig, E. T. and J. M. Waters. (1994) *Track geotechnology and substructure management*, Thomas Telford, London,.

Rowe PK and Jones CJFP 2000. *Geosynthetics: innovative materials and rational design*, Proceedings of the International Conference on Geological and Geotechnical Engineering, GeoEngineering-2000, Vol. 1, Melbourne, Australia:1124-1156, 2000.

Indraratna B, Nimbalkar S, Christie D, Rujikiatkamjorn C and Vinod JS. *Field assessment of the performance of a ballasted rail track with and without geosynthetics.* Journal of Geotechnical and Geoenvironmental Engineering, ASCE, 136(7): 907–917, 2010.

Indraratna, B., W. Salim and C. Rujikiatkamjorn. *Advanced Rail Geotechnology - Ballasted Track*, CRC Press, Taylor & Francis Group, London, UK, 2011a.

Indraratna, B., N.T. Ngo and C. Rujikiatkamjorn. *Behavior of geogrid-reinforced ballast under various levels of fouling*. Geotextiles and Geomembranes 29(3): 313-322, 2011b.

Rail Infrastructure Corporation of NSW. *Specification for supply of aggregates for ballast.* TS 3402, Sydney, Australia, 2001.

Indraratna, B., N.T. Ngo and C. Rujikiatkamjorn. (2013) *Studying the deformation of coal fouled ballast stabilised with geogrid under cyclic load*. Journal of Geotechnical and Geoenvironmental Engineering-ASCE 139(8): 1275–1289,.

Indraratna, B., M. M. Biabani and S. Nimbalkar. *Behavior of geocell-reinforced subballast subjected to cyclic loading in plane-strain condition*. Journal of Geotechnical and Geoenvironmental Engineering 141(1): 04014081, 2015.

Marschnig, S., and Veit, P. (2011). *Making a case for under sleeper pads.* Intl. Railway Journal, 51(1), 27-29.

Mcinnes, D. B. (1986). *Drying effect of different verge planted tree species on urban roads*. 13 ARRB and 5th REAAA Conference, 54-66.

Ngo, N.T., B. Indraratna, C. Rujikiatkamjorn and M. M. Biabani. *Experimental and discrete element modeling of geocell-stabilized subballast subjected to cyclic loading*." Journal of Geotechnical and Geoenvironmental Engineering 142(4): 04015100, 2016.

Ngo, N.T., B. Indraratna and C. Rujikiatkamjorn. *DEM simulation of the behaviour of geogrid stabilised ballast fouled with coal*. Computers and Geotechnics 55: 224-231, 2014.

Ni J (2012). Application of geosynthetic vertical drains under cyclic loads in stabilizing track. PhD thesis, Centre for GRE, University of Wollongong, Australia.

Nimbalkar, S., Indraratna, B., Dash, S., and Christie, D. (2012). *Improved Performance of Railway Ballast under Impact Loads Using Shock Mats.* Journal of Geotechnical and Geoenvironmental Engineering, 138(3), 281-294.

Schneider, P., Bolmsvik, R., and Nielsen, J. C. O. (2011). *In situ performance of a ballasted railway track with under sleeper pads*. Proceedings of the Institution of Mechanical Engineers, Part F: Journal of Rail and Rapid Transit, 225(3), 299-309.

Sivakumar V, Jeludine DKNM, Bell A, Glynn DT, Mackinnon P (2011). *The pressure distribution along stone column in soft clay under consolidation and foundation loading.* Géotechnique 61(7), 613 - 620.

Tasalloti, S.M.A., Indraratna, B., Rujikiatkamjorn, C., Heitor, A. and Chiaro, G. (2015a). A laboratory study on the shear behavior of mixtures of coal wash and steel furnace slag as potential structural fill, Geotechnical Testing Journal, 38(4), 1-12.

Tasalloti, S.M.A., Indraratna, B., Chiaro, G. and Heitor, A. (2015b): Field investigation on compaction and strength performance of two coal wash-BOS slag mixtures, ASCE Geotechnical Special Publication, 256, 2359-2368 (Proc. of the 2015 International Foundations Congress. & Equipment Expo,, 17-21 March 2015, San Antonio, Texas, USA).

Wang, G. (2010). Determination of the expansion force of coarse steel slag aggregate. Construction and Building Materials 24(10): 1961-1966.